Ang II Enhances Atrial Fibroblast Autophagy and Promotes Atrial Remodeling Through the AT1-ERK-mTOR Signaling Pathway

Xudong Xu
Zhejiang University School of Medicine Sir Run Run Shaw Hospital
Mengmeng Chen
Zhejiang University School of Medicine Sir Run Run Shaw Hospital
Hangyuan Qiu
Zhejiang University School of Medicine Sir Run Run Shaw Hospital
Kuangshi Zhou
Zhejiang University School of Medicine Sir Run Run Shaw Hospital
Jun Zhu
Zhejiang University School of Medicine Sir Run Run Shaw Hospital
Hui Cheng
Zhejiang University School of Medicine Sir Run Run Shaw Hospital
Yunhe Wang
Zhejiang University School of Medicine Sir Run Run Shaw Hospital
Guosheng Fu
Zhejiang University School of Medicine Sir Run Run Shaw Hospital
Ruhong Jiang
Zhejiang University School of Medicine Sir Run Run Shaw Hospital
Chenyang Jiang (cyjiang@zju.edu.cn)
Sir run run shaw hospital, zhejiang university

Original investigation

Keywords: Ang II, Atrial remodeling, Autophagy, Atrial fibroblast, Collagen

Posted Date: August 4th, 2020

DOI: https://doi.org/10.21203/rs.3.rs-42393/v1

Abstract

Background: Atrial remodeling is a common pathological change in atrial fibrillation (AF), while the mechanism of atrial remodeling remains unclear. In the present study, we investigated the autophagy and collagen secretion in atrial fibroblasts in response to renin-angiotensin system (RAS) activation and elucidated the relationship between atrial fibroblast autophagy and atrial remodeling.

Methods: Right atrial tissues was obtained from patients that underwent cardiac valve replacement after signed the informed consent form. In vivo, subcutaneous perfusion of angiotensin II (Ang II) was used to mimic activation of the RAS and induce atrial remodeling. Electrical remodeling and AF induction were assessed by electrophysiology and programmed stimulation. In vitro, atrial fibroblasts were isolated and cultured. Autophagic flux changes were assessed by mCherry-GFP-LC3 adenovirus transfection. All samples were collected, collagen expression, autophagy changes and atrial remodeling were evaluated by western blot, masson's trichrome staining, immunohistochemistry and immunofluorescence mainly.

Results: Atrial tissue samples from patients with atrial fibrillation showed more collagen deposition and enhanced autophagy than those with sinus rhythm. Chronic subcutaneous Ang II perfusion in mice promoted atrial remodeling and susceptible to AF induction. In cultured atrial fibroblasts, the expression of collagen I (COL-I) and collagen III (COL-III) and autophagy both increased when cells were treated with Ang II, and the autophagic flux was enhanced by Ang II. However, blocking autophagy reduced the expression of COL-I and COL-III. Besides, Ang II induced the phosphorylation of ERK and suppressed the phosphorylation of mTOR. In contrast, inhibition of the angiotensin II type 1 receptor (AT1) or ERK signaling pathway not only suppressed the autophagy induced by Ang II but also reduced COL-I and COL-III expression.

Conclusions: In summary, these results suggest that Ang II promotes autophagy in atrial fibroblasts, which aggravates atrial remodeling and increases the susceptibility to AF induction. Autophagy may be a potential target for relieving atrial remodeling and AF after RAS activation.

1. Introduction

Atrial fibrillation (AF) is one of the most common tachyarrhythmia in clinical practice, which can induce heart failure and stroke[1]. At present, the treatment of AF focuses on rhythm control, rate control and anti-coagulation. However, both of them only relieve symptoms and decrease the incidence of stroke, while the alteration of atrial substrate is ongoing and leads to AF that is difficult to cure and easy to relapse. The mechanism of AF is complicated, and atrial remodeling is a key point from the perspective of pathophysiology[2]. Electrical remodeling occurs in the early stage of AF, while structural remodeling, such as extracellular matrix (ECM) deposition, occurs as AF progresses. The abnormal ECM production and degradation lead to atrial interstitial fibrosis, which has been verified to aggravate the development of AF[3, 4]. The deposition of collagen in the atrial interstitium not only causes atrial structural changes but also affects electrical conduction[5]. Therefore, improving atrial remodeling is a pivotal part in the treatment of AF.

Autophagy, an evolutionarily conserved metabolic process in eukaryotes, has three types: chaperone-mediated autophagy, microautophagy, and macroautophagy[6]. Macroautophagy (hereafter known as autophagy), which is carried out by autophagosomes, is the major type that helps to eliminate damaged organelles and proteins. Normally, autophagy occurs at a basic level in various cells and organs to maintain homeostasis. However, factors such as starvation, absence of energy, growth factors, infection and oxidative stress induce autophagy dysfunction[7]. Increasing studies have reported that autophagy has an important role in ischemia-reperfusion, heart failure, cardiac fibrosis, atherosclerosis and AF[8–10]. Recently, researchers have detected excessive autophagy in cardiac hypertrophy and heart failure[11–13]. Wiersma *et al.* reported that autophagy and endoplasmic reticulum stress were enhanced in AF patients' atrial tissue. Inhibition of autophagy improved atrial electrical remodeling[14].

Previous studies have reported that the renin-angiotensin system (RAS) activated in cardiovascular diseases, including hypertension, heart failure, cardiac hypertrophy and AF[15–17]. It is documented that RAS plays a critical role in the initiation and development of AF. The incidence of AF was decreased after myocardial infarction when patients were treated with angiotensin-converting enzyme inhibitors[18]. In addition, in a dog AF model that led to heart failure, the animals exhibited serious atrial interstitial fibrosis and atrial conduction dysfunction. Meanwhile, they had a higher angiotensin II (Ang II) content in the atrium. Interestingly, enalapril reversed these changes[19]. Ang II is the main effector when RAS is activated, playing an important role in cell growth and proliferation, cell differentiation, inflammation and fibrogenesis[20, 21]. Ang II has been reported to facilitate interstitial fibrosis and atrial remodeling, causing AF[22, 23]. Porrello *et al.* reported that Ang II promoted autophagy in neonatal cardiomyocytes through angiotensin II receptor type 1 (AT1)[24]. Ang II also causes cardiac remodeling by promoting fibroblast proliferation and cardiomyocyte hypertrophy[2].

Altogether, these studies suggest that a relationship may exist between autophagy and AF. We previously found that Ang II induced collagen I (COL-I) and collagen III (COL-III) secretion in atrial fibroblasts. Therefore, in the present study, we aimed to assess whether autophagy is activated in persistent AF patients' atrial tissue. Then, we investigated the role of atrial fibroblast autophagy induced by Ang II in atrial remodeling and illuminated the potential mechanism.

2. Materials And Methods

2.1 Reagents and antibodies

Cell culture medium (DMEM basic) was purchased from Gibco (Shanghai, China). Ang II was purchased from Bachem (Bubendorf, Switzerland). Fetal bovine serum (FBS) was obtained from GEMINI (Woodland, CA). Rapamycin (Rapa), LY294002 and candesartan (Can) were purchased from Selleck Chemicals (Huston, Texas). Elisa kit for human Ang II was purchased from Enzo life science (New York, USA). Masson's trichrome staining kit was purchased from Solarbio (Beijing, China). siRNAs and transfection reagent were from Ribo-Bio (Guangzhou, China). DAPI staining solution (C1005) and protease inhibitor (ST506) were purchased from Beyotime (Shanghai, China). Cell lysis buffer was purchased from

cytoskeleton (Denver, Colorado). Phosphatase inhibitors were purchased from Roche (Basel, Switzerland). mCherry-GFP-LC3 was purchased from ViGene (Jinan, China). Antibodies for collagen III (COL-III, ab7778), p62/SQSTM1 (ab109012) and AT1 (ab124734) were purchased from Abcam (Cambridge, UK). Collagen I antibody (COL-I, GTX20292) was purchased from GeneTex (California, USA). Beclin 1 antibody (11306-1-AP) was purchased from Proteintech (Wuhan, China). Vimentin antibody (EM0401) was purchased from Huabio (Hangzhou, China). Phospho-mTOR (2971), mTOR (2972), phospho-ERK (4370) and ERK (4377) antibodies were purchased from Cell Signaling Technology (Boston, Massachusetts). LC3-II antibody (L7543), DMSO and chloroquine diphosphate salt (CQ) were purchased from Sigma (St. Louis, USA). 3-methyladenine (3-MA), candesartan cilexetil and PD98059 were from MedChemExpress (Monmouth, NJ). GAPDH antibody (ab011-100), goat anti-rabbit (GAR007) and goat anti-mouse (GAM007) horseradish peroxidase (HRP)-IgG were obtained from Multi Sciences (Hangzhou, China). TRITC-conjugated goat anti-rabbit antibody (A16115) and Alexa 488-conjugated goat anti-mouse antibody (A-11001) were purchased from Thermo Fisher Scientific.

2.2 Human atrial tissue

Right atrial tissues were obtained from patients who underwent cardiac valve replacement. All patients and at least one family member of each donor signed the informed consent form. The application for collecting and using human samples for science research was approved by the Human Research Ethics Committee of Sir Run Run Shaw Hospital of Zhejiang University. This human sample study conformed to the Declaration of Helsinki. The exclusion criteria included hypertension, heart failure, coronary artery diseases, hyperthyroidism, systemic inflammatory diseases, malignancy and history of angiotensin-converting enzyme inhibitors or angiotensin receptor blockers. Sixteen patients with sinus rhythm and sixteen patients with persistent AF (> 6 months) were enrolled, and their right atrial tissues were obtained. The atrial tissue was collected and cleaned in ice-cold normal saline. Each sample was divided into two parts. One was fixed with 4% paraformaldehyde for histological analysis, and the other was saved at -80℃ for RNA and protein extraction. The baseline characteristics of these patients are described in Table 1.

Table 1
Baseline characteristics of the patients.

	SR(n = 16)	AF(n = 16)
Age(years)	55.88 ± 2.62	58.94 ± 2.16
Gender(female)	6(37.50%)	9(56.25%)
Body weight(kg)	63.75 ± 4.11	66.28 ± 3.81
Heart rate(bpm)	80.69 ± 3.07	101.80 ± 6.46**
Systolic pressure(mmHg)	117.90 ± 4.40	
Diastolic pressure(mmHg)	73.81 ± 2.89	
Dyslipidemia	1(6.25%)	
Diabetes mellitus	6(37.5%)	
Echocardiographic indicators		121.10 ± 4.00
LAD (mm)	45.19 ± 2.01	77.69 ± 3.85
LVID-d (mm)	54.80 ± 2.02	1(6.25%)
IVS-d (mm)	11.08 ± 0.58	0(0%)
LVPW-d (mm)	11.16 ± 0.47	
LVEF (%)	61.67 ± 2.39	56.84 ± 2.62**
		54.15 ± 2.12
		10.13 ± 0.37
		9.30 ± 0.36**
		62.46 ± 2.46

SR: sinus rhythm; AF: atrial fibrillation; LAD: left atrial diameter; LVID-d: left ventricular internal diameter at end-diastole; IVS-d: interventricular septum at end-diastole; LVPW-d: left ventricular posterior wall at end-diastole; LVEF: left ventricular ejection fraction. Data are expressed as the mean ± SEM; n = 16 each group. **p < 0.01 vs SR group (SR).

2.3 Enzyme-linked immunosorbent assay (ELISA)

The patient's central venous blood was taken and centrifuged immediately. Human serum was saved at -80℃. The concentration of Ang II in serum was measured by ELISA following the manufacturers' instructions.

2.4 Animal experiment

All animal experiments in the present study were approved by the Institutional Animal Care and Use Committee of Zhejiang University and conducted in accordance with the National Institutes of Health Guide for the Care and Use of Laboratory Animals. Male C57BL/6 mice at the age of 8 weeks (provided by the experimental animal center of Sir Run Run Shaw Hospital) were fed a chow diet in a 12-hour light/12-hour dark environment at 25 °C in the experimental animal center of Sir Run Run Shaw Hospital. Forty-five mice were randomly divided into 5 groups: the control group with normal saline-infused, Ang II-infused group (1.6 mg/kg/day), autophagy-enhanced group with intraperitoneal injection of Rapa (1.5 mg/kg/day) and Ang II perfusion (1.6 mg/kg/day), autophagy-inhibited group with intraperitoneal injection of 3-MA (35 mg/kg/day) and Ang II perfusion (1.6 mg/kg/day), and candesartan-treated group with oral administration of candesartan cilexetil (5 mg/kg/day) and Ang II perfusion (1.6 mg/kg/day). Subcutaneous perfusion of Ang II was used to mimic activation of the RAS and induce atrial remodeling. In brief, mice were anesthetized with 0.3% sodium pentobarbital solution firstly. Then, prepared osmotic minipumps (Alzet, model of 2004; Alzet Corp) were subcutaneously implanted in the right intrascapular area of mice. Each pump contained normal saline (for the control group only) or Ang II (1.6 mg/kg/day for 28 days). The velocity of perfusion was 0.25 μl/hour. After 28 days of treatment, mice were subjected to transthoracic echocardiographic and electrophysiological detection in vivo.

2.5 Echocardiography

Mice were anesthetized by isoflurane, and echocardiography was performed using a Vevo 1100 ultrasound system (Visual Sonics, Toronto, Canada) with a 30 MHz transducer as previously described[25]. M-mode images were obtained from a parasternal short-axis view. The parameters measured were as follows: heart rate (HR), interventricular septum at end-diastole (IVS-d), interventricular septum at end-systole (IVS-s), left ventricular posterior wall at end-diastole (LVPW-d), left ventricular posterior wall at end-systole (LVPW-s), left ventricular internal dimensions at end-diastole (LVID-d) and left ventricular internal dimensions at end-systolic (LVID-s). Left ventricular ejection fraction (LVEF) and left ventricular fractional shortening (LVFS) were calculated. All measurements were averaged from at least three consecutive cardiac cycles.

2.6 In vivo electrophysiology and programmed stimulation

The electrophysiology and programmed stimulation in vivo were done as previously described[26, 27]. In brief, mice were anesthetized with 0.3% sodium pentobarbital solution and a subcutaneous administration of 0.03 mg/kg buprenorphine hydrochloride to relieve pain. The subdermal needle electrodes were placed in the legs to make a lead II conformation. The right external jugular vein was separated carefully, and a 1.1 F electrophysiology catheter, which included eight electrodes (Transonic Scisense, Canada), was inserted into the right atrium through the jugular vein. The surface electrocardiogram (ECG) and intracardiac ECG were observed. The correct catheter position was ensured by obtaining a sole ventricular signal in the distal lead and a predominant atrial signal in the proximal lead. The atrial effective refractory period (AERP) was determined by applying eight training stimuli (S1) at a cycle length of 100 ms, followed by an extra stimulus (S2). The S1-S2 interval was progressively reduced by 2 ms in each pacing train from 70 ms. AERP was defined as the longest S1-S2 coupling

interval for atria that failed to generate a propagated beat with S2. After each stimulation protocol, there was a recovery period of at least 30 seconds. AF inducibility was tested by a burst pacing protocol in the right atrium. In other words, three trains of 2 s burst pacing were used as follows: the first 2 s burst was given at a cycle length of 40 ms with a pulse duration of 5 ms. Then, mice stabilized for 3 minutes. The second 2 s burst pacing was set as a cycle length of 20 ms with a pulse duration of 5 ms. Another 3 minutes of stabilization applied. The last 2 s burst pacing was applied at a cycle length of 20 ms with a pulse duration of 10 ms. AF was defined as irregular R-R intervals without P waves for at least 1 s on the surface electrocardiogram (ECG). All data were acquired by a cardiac electrophysiology stimulator and a multichannel electrophysiological recording system (Transonic Scisense, Canada). All animals were sacrificed by cervical dislocation when the experiment finished.

2.7 Masson's trichrome staining

Human and mouse atrial tissues were embedded in paraffin after fixation with 4% paraformaldehyde solution and sliced into 4-μm-thick sections. Tissue sections were stained with Masson's trichrome according to the manufacturer's instructions. Microscopy images were captured by Leica image analysis software (Leica, Germany). The atrial interstitial fibrotic areas were calculated by Image-Pro Plus software (version 6.0; Media Cybernetics, USA). The collagen volume fraction was calculated as collagen area/total area·100%.

2.8 Immunohistochemistry

Mouse atrium was harvested and fixed with 4% paraformaldehyde solution. Paraffin-embedded tissues were cut into 4-μm-thick sections. Immunohistochemical staining was performed using the antibodies for COL-I and COL-III (1:200) at 37℃ for 1 hour and then secondary antibody at 37℃ for 30 min. Then, the sections were visualized with a DAB (Gene Tech, China) method. Microscopy images were captured by Leica image analysis software (Leica, Germany).

2.9 Immunofluorescence Staining

Atrial tissue sections were stained with antibodies for LC3-II (1:50) and vimentin (1:100) overnight at 4℃. TRITC-conjugated goat anti-rabbit antibody and Alexa 488-conjugated goat anti-mouse antibody (1:500) were applied as secondary antibodies and incubated for 2 hours at 37℃. Cell nuclei were stained with DAPI for 10 min at room temperature. All fluorescence images were captured by laser scanning confocal microscopy (Nikon, Japan) under the same conditions.

2.10 Quantitative real-time polymerase chain reaction (Q-PCR)

The RNA of human atrial tissues (100 mg) was extracted by using Trizol (Invitrogen, Carlsbad, USA) according to the manufacturer's instructions. cDNA was synthesized using a reverse transcription kit (Takara, Dalian, China) and used for subsequent qPCR. All samples were measured in triplicate. Differences in gene expression were calculated using the $2^{-(\triangle\triangle CT)}$ method. The primers for the measured genes were as follows: GAPDH: F-5'-GCACCGTCAAGGCTGAGAAC-3', R-5'-TGGTGAAGACGCCAGTGGA-3';

COL-I: F-5’-GGACACAGAGGTTTCAGTGGT-3’, R-5’-AGTAGCACCATCATTTCCACGA-3’; COL-III: F-5’-CGCCCTCCTAATGGTCAAGG-3’, R-5’-TTCTGAGGACCAGTAGGGCA-3’. GAPDH was used as an internal reference gene.

2.11 Cell culture

Atrial fibroblasts were isolated from mouse atria, as previously described[28, 29]. Cell culture was followed the methods of Xu *et al.* 2019[30]. For chemical stimulations, cells were pretreated with different concentrations of rapamycin, LY294002, CQ, PD98059 or candesartan for 1 hour and induced with Ang II (10^{-6} μM) for 48 hours. For phosphorylated protein measurements, cells were pretreated with PD98059 (10 μM) and candesartan (10 μM) for 1 hour and stimulated with Ang II for 20 min, and cells were harvested for protein detection.

2.12 Small interfering RNA transfection

Small interfering RNAs (siRNA) targeting Beclin 1 and AT1 and their corresponding negative control siRNAs were designed and synthesized by Ribo-Bio corporation (Guangzhou, China). The sequences were as follows: Beclin 1: 5’-GGCACAATCAATAATTTCA-3’; AT1: 5’- CCTACTCTCTACAGCATCA-3’. Cells were seeded in 6-well dishes, and a transfection experiment was conducted when cells reached 30% confluence. siRNA (100 nM) and transfection reagent (Ribo-Bio Corporation, Guangzhou, China) were mixed and incubated for 10 min at room temperature according to the manufacturer's recommendations. The mixed reagent was added into each well. Negative-control siRNAs were used in the experiment. The effect of siRNA was assessed by q-PCR and Western blot. After transfection, atrial fibroblasts were stimulated with Ang II similarly to previous experiments in this study.

2.13 Ad-mCherry-GFP-LC3 transfection

To observe autophagic flux changes induced by Ang II, atrial fibroblasts were transfected with mCherry-GFP-LC3 adenovirus as described previously[30]. Cells were pretreated with candesartan, PD98059 or siRNA (targeting AT1) as described above and then stimulated with Ang II. At that time, the cells were fixed with 4% paraformaldehyde. Cell nuclei were stained with DAPI for 10 min at room temperature. Images were captured by laser scanning confocal microscopy (Nikon, Japan) under the same conditions. The average numbers of red and yellow puncta (merged channel) from 30 atrial fibroblasts in each group were counted manually in five independent experiments. Autophagosomes, which express both green and red fluorescence, appeared yellow, and autolysosomes appeared only red because GFP was degraded under acidic conditions.

2.14 Western blot analysis

Western blot analysis was followed the methods of Xu *et al.* 2019[30]

2.15 Statistical analysis

The data analysis was conducted using GraphPad Prism 7.0 (GraphPad Software, San Diego, CA, USA). Normal distribution data are expressed as the mean ± standard error of the mean (SEM). Abnormal distribution data are expressed as median and interquartile range by nonparametric test (Mann-Whitney test). Comparisons between two groups were performed with an unpaired student *t* test. Comparisons more than two groups were performed using one-way ANOVA followed by Bonferroni correction. Fisher's exact test was applied to compare AF inducibility. $P < 0.05$ was regarded as statistically significant.

3 Results

3.1 Enhanced autophagy and more serious interstitial fibrosis in AF patients' atrial tissues

Persistent activation of RAS promotes atrial fibrosis and increases the susceptibility to AF. In the present study, we collected the atrial tissue of sinus rhythm and atrial fibrillation patients. First, we tested the concentration of Ang II in patients' serum. As shown in Fig. 1e, the concentration of Ang II was higher in the AF group than in the SR group. Masson's trichrome staining showed heavier collagen deposition in the atrial interstitial in the AF group, and the collagen volume infraction was approximately 26.7% in the AF group and 19.5% in the SR group (Fig. 1a). We examined the expression of COL-I and COL-III and autophagy markers in two groups of atrial tissues. Both COL-I and COL-III had higher expression in the AF group compared to the SR group at the protein and mRNA levels (Fig. 1b, 1c and 1d), which was consistent with the Masson's trichrome staining results. The expression of LC3-II and Beclin 1 was increased in the AF group, in contrast, the expression of p62 was decreased in the AF group. These changes suggested that autophagy was activated in the AF patients. Further, we found a higher expression of COL-I and COL-III and increased autophagy in AF patients compared to SR patients. Therefore, we speculated that there may be a potential relationship between atrial fibrosis and autophagy.

3.2 Role of autophagy and AT1 in Ang II-induced cardiac remodeling and dysfunction in vivo

Consecutive perfused of Ang II was used to mimic the effect of RAS activation. Cardiac remodeling was evaluated by echocardiography preliminary. The results showed that IVS-d was increased when mice were perfused with Ang II. However, the increased IVS-d was relieved when autophagy was suppressed with 3-MA or AT1 was blocked with candesartan compared to the Ang II group. Similarly, Ang II perfusion with or without rapamycin decreased the LVEF and LVFS, but these were upregulated in groups treated with 3-MA or candesartan, although not significantly in the autophagy-inhibited group (3-MA + Ang II) compared to the Ang II group. Additionally, the ratio of heart weight to body weight (HW/BW) was increased in the Ang

II and autophagy-enhanced (Rapa + Ang II) groups. 3-MA and candesartan both suppressed the increase in HW/BW induced by Ang II (Table 2). These results indicate that consecutive perfusion with Ang II promoted cardiac remodeling and dysfunction. In contrast, inhibiting autophagy or blocking AT1 both improved the cardiac dysfunction induced by Ang II.

Table 2
Heart weight/body weight ratio and echocardiographic parameters.

Control	Ang II	Rapa + Ang II	3-MA + Ang II	Can + Ang II	
HW/BW (mg/g)	5.52 ± 0.28	6.63 ± 0.09**	6.60 ± 0.28**	5.85 ± 0.14&	5.71 ± 0.09&&
HR (bpm)	481.5 ± 14.09	488.4 ± 13.17	475.5 ± 20.21	465.5 ± 6.013	473.2 ± 12.25
IVS-d(mm)	0.84 ± 0.04	1.05 ± 0.03*	0.92 ± 0.07	0.81 ± 0.07&	0.77 ± 0.06&&
IVS-s(mm)	1.29 ± 0.08	1.38 ± 0.08	1.27 ± 0.08	1.30 ± 0.14	1.23 ± 0.09
LVPW-d(mm)	0.75 ± 0.05	0.82 ± 0.04	0.81 ± 0.07	0.75 ± 0.04	0.72 ± 0.04
LVPW-s(mm)	1.10 ± 0.05	1.06 ± 0.04	1.02 ± 0.10	1.02 ± 0.06	1.09 ± 0.05
LVEF%	56.78 ± 2.96	47.17 ± 2.01*	43.79 ± 3.43**	55.66 ± 1.06	56.82 ± 2.07&
LVFS%	29.74 ± 1.89	22.82 ± 1.05**	22.38 ± 2.12**	28.85 ± 0.73&	29.15 ± 1.33&

Rapa: rapamycin; 3-MA: 3-methyladenine; Can: candesartan; HW/BW: heart weight/body weight; HR: heart rate; IVS-d: interventricular septum at end-diastole; IVS-s: interventricular septum at end-systole; LVPW-d: left ventricular posterior wall at end-diastole; LVPW-s: left ventricular posterior wall at end-systole; LVEF: left ventricular ejection fraction; LVFS: left ventricular fraction shortening. Data are expressed as the mean ± SEM; n = 9 each group. *$p < 0.05$ vs control group (Control); **$p < 0.01$ vs control group; &$p < 0.05$ vs Ang II group (Ang II); &&$p < 0.01$ vs Ang II group.

3.3 Inhibiting autophagy or blocking AT1 reduces the susceptibility to AF induction and improves the atrial electrical remodeling induced by Ang II

Atrial electrical remodeling occurs in the early stage of AF, which manifests as a reduced AERP, reduced action potential duration and changes in ion channels in cell membrane such as L-type calcium channels, Na^+ channels and K^+ channels[31, 32]. In this study, we detected AERP and AF inducibility in vivo. As shown in Fig. 2b, the rate of AF inducibility was increased when the mice were perfused with Ang II with or without Rapa. In contrast, the rate of AF inducibility was decreased in the autophagy inhibition group (3-MA + Ang II). We also found that the rate of AF inducibility was reduced when AT1 was inhibited by candesartan (Can). Shortened AERP contributed to the formation of reentry and led to AF occurrence. In this study, the electrophysiological examination showed that AERP was shortened in the Ang II- and autophagy-enhanced groups (Rapa + Ang II); however, this change was reversed when autophagy was

repressed by 3-MA or AT1 was blocked by candesartan (Fig. 2c). That is, inhibition of autophagy or AT1 improves the atrial electrical remodeling and reduced the AF inducibility induced by Ang II.

3.4 Inhibiting autophagy or blocking AT1 reverses the deposition of collagen and the expression of COL-I and COL-III in the mouse atrium induced by Ang II.

Collagen deposition in atrial interstitium not only accelerates atrial structural remodeling but also causes abnormal atrial electrical conduction. To investigate collagen deposition in the atrial interstitium induced by Ang II, we detected the collagen volume fraction (CVF) by Masson's trichrome staining. The results showed that CVF was increased in Ang II with or without rapamycin. 3-MA, as an autophagy inhibitor, reduced CVF. That is, blocking autophagy reduced the collagen production induced by Ang II. Additionally, blocking AT1 with candesartan also decreased CVF, which implied that Ang II induced collagen secretion through AT1 (Fig. 3a and 3b). Meanwhile, we analyzed the expression of COL-I and COL-III in the mouse atrium. Similar to CVF, Ang II increased the expression of COL-I and COL-III in the atrium. Enhancing autophagy with Rapa (Rapa + Ang II) also upregulated COL-I and COL-III. However, the expression of COL-I and COL-III were both decreased when mice were treated with 3-MA, an autophagy inhibitor, or candesartan, an AT1 antagonist (Fig. 3c). Taken together, these results suggest that Ang II promoted collagen deposition in atrium. Inhibiting autophagy or blocking AT1 both reduced collagen production and ameliorated atrial remodeling induced by Ang II.

3.5 Candesartan relieves atrial fibroblast autophagy that is induced by Ang II in mice.

The proportion of heart cells that are fibroblasts is approximately 40%-60%, and fibroblasts are the main cell type that secretes collagen[33]. The role of fibroblasts is important in cardiac fibrosis and has attracted the attention of researchers[34, 35]. To detect changes in atrial fibroblast autophagy when mice were perfused with Ang II, double immunofluorescence staining of sections from mice atrium was used. Atrial fibroblasts were labeled with vimentin, a fibroblast marker, and LC3-II was stained to reflect autophagy. As shown in Fig. 4, the expression of LC3-II was increased in vimentin-positive atrial fibroblasts in the Ang II group and autophagy-enhanced group (Rapa + Ang II) compared to the control group. However, the increased expression of LC3-II was relieved when autophagy was inhibited by 3-MA or AT1 was blocked by candesartan. These results indicate that Ang II activated atrial fibroblast autophagy, which was inhibited by candesartan, an AT1 antagonist, and that Ang II-induced atrial fibroblast autophagy may occur through AT1.

3.6 Ang II promotes the expression of COL-I and COL-III and activates autophagy in atrial fibroblasts.

Ang II is the major effector of RAS, which plays an important role in cardiovascular diseases, including hypertension, cardiac remodeling and interstitial fibrosis[36]. COL-I and COL-III, the primary ingredient of

the extracellular matrix, are regarded as the key biomarkers of cardiac fibrosis[37]. In this study, the expression of both COL-I and COL-III by atrial fibroblasts was increased in response to Ang II stimulation (Fig. 5a and 5b). On the other hand, we found that Ang II also elevated the expression of LC3-II, and decreased the expression of p62 in cultured atrial fibroblasts (Fig. 5c and 5d). That is, Ang II activated autophagy in atrial fibroblasts. These results suggest that Ang II, an effector of RAS, upregulated autophagy and promoted COL-I and COL-III secretion in atrial fibroblasts.

3.7 Atrial fibroblast autophagy is positively correlated with the expression of COL-I and COL-III.

The preceding results suggested that Ang II-stimulated COL-I and COL-III expression accompanied increased autophagy in atrial fibroblasts. To clarify whether atrial fibroblast autophagy was associated with COL-I and COL-III expression. Rapamycin (Rapa), a mammalian target of rapamycin (mTOR) inhibitor, is widely used as an autophagy inducer. Ang II upregulated the expression of COL-I and COL-III in atrial fibroblasts. Intriguingly, the expression of COL-I and COL-III was further evaluated when cells were pretreated with rapamycin compared to Ang II stimulation alone (Fig. 6a and 6d). As expected, COL-I and COL-III was downregulated when autophagy was curbed by CQ, a lysosome acidification inhibitor (Fig. 6b and 6e). To confirm this effect, LY294002, a PI3-kinase inhibitor, which also inhibits autophagy, was used. In alignment with the CQ results, the expression of both COL-I and COL-III both decreased when atrial fibroblasts were pretreated with LY294002 (Fig. 6c and 6f). Beclin 1 is a pivotal gene in the initial autophagy process. Therefore, we designed a small interfering RNA targeted to Beclin 1 to disturb the process of autophagy. In agreement with the pharmacological experiment, atrial fibroblast autophagy induced by Ang II was inhibited, and the expression of both COL-I and COL-III was reduced when fibroblasts were treated with siRNA targeted to Beclin 1 (Fig. 6g, 6 h and 6i). These results confirm that Ang II stimulated COL-I and COL-III secretion by activating autophagy, and this effect was reversed apparently when atrial fibroblast autophagy was suppressed.

3.8 Blocking ERK signaling reduces the expression of COL-I and COL-III and inhibits atrial fibroblast autophagy induced by Ang II by upregulating the phosphorylation of mTOR.

Extracellular signal-regulated kinase (ERK) is associated with cell proliferation and differentiation, which is a regulator of autophagy[38, 39]. We found that the phosphorylation of ERK was increased when atrial fibroblasts were stimulated with Ang II. PD98059, a specific inhibitor of ERK, not only reduced the expression of COL-I and COL-III but also suppressed atrial fibroblast autophagy (Fig. 7a and 7b). mTOR is the most important target of autophagy regulation, in which it acts as a negative regulator[40]. In the present study, we found that phosphorylation of mTOR was decreased under stimulation with Ang II. Interestingly, this variation was rescued when atrial fibroblasts were pretreated with PD98059 (Fig. 7c and 7d). This indicated that enhanced autophagy in atrial fibroblasts induced by Ang II may be related to the ERK signaling pathway.

3.9 Blocking AT1 reduces the expression of COL-I and COL-III and suppresses atrial fibroblast autophagy induced by Ang II through the ERK-mTOR signaling pathway.

Ang II affects the cardiovascular system predominantly via AT1. A previous study reported that the angiotensin II receptor acted as a regulator of autophagy in cardiomyocytes[24]. Therefore, we investigated whether Ang II-induced autophagy in atrial fibroblasts relied on AT1. As expected, the expression of both COL-I and COL-III induced by Ang II was decreased when atrial fibroblasts were pretreated with candesartan, a specific AT1 antagonist. Moreover, autophagy was inhibited, as reflected by the decreased expression of LC3-II and increased expression of p62 (Fig. 8a and 8b). Furthermore, candesartan alleviated the phosphorylation of ERK and enhanced the phosphorylation of mTOR (Fig. 8c and 8 g). To further verify the effect of AT, the siRNA targeted to AT1 was designed and transfected to knockdown AT1 (Fig. 8f). Results consistent with the candesartan stimulation were acquired. The knockdown of AT1 reduced COL-I and COL-III production and inhibited fibroblast autophagy induced by Ang II (Fig. 8e and 8 h). Besides, ERK phosphorylation declined and mTOR phosphorylation elevated when AT1 was silenced (Fig. 8d and 8i). In summary, Ang II induced collagen secretion and autophagy activation through AT1. Blocking AT1 contributed to improving collagen production and atrial interstitial fibrosis.

3.10 Ang II induces autophagic flux in atrial fibroblasts which is reversed by PD98059 and AT1 disturbance.

To further investigate the complex influences of AT1 and the ERK signaling pathway on autophagy, a special marker, mCherry-GFP-LC3, was utilized in an adenovirus. Cultured atrial fibroblasts were transfected with the adenovirus for 24 hours. Then, cells were stimulated with Ang II or pretreated with candesartan or PD98059 for 1 hour before stimulation with Ang II. As shown in Fig. 9, yellow puncta represent autophagosomes, and red puncta represent lysosomes in the merged channel. The yellow and red puncta were conspicuously augmented when fibroblasts were stimulated by Ang II, which represented the enhanced autophagic flux. As expected, the enhanced autophagic flux was suppressed when cells were pretreated with candesartan and PD98059. A similar result was obtained when AT1 was silenced by siRNA. These results reflect the variation of atrial fibroblast autophagic flux dynamically and directly. They also verify the autophagy alteration in atrial fibroblasts.

4. Discussion

In the present study, we demonstrated the relationship between autophagy and AF, and the principal discoveries were as follows: first, compared to SR patients, more significant collagen deposition and enhanced autophagy were detected in AF patients' atrial tissues. Second, overloaded Ang II aggravates atrial remodeling and AF inducibility in vivo, and enhances fibroblast autophagy. Meanwhile, blocking

autophagy or antagonizing AT1 can relieve atrial remodeling and reduced AF inducibility. Third, Autophagic flux was also increased in response to Ang II. The enhanced autophagy was a positive-feedback response to Ang II stimulation. In contrast, secretion of COL-I and COL-III was reduced when autophagy was restrained. Moreover, the results showed that Ang II induced autophagy through the AT1-ERK-mTOR signaling pathway in atrial fibroblasts. Antagonists targeted to AT1 and ERK both upregulated the phosphorylation of mTOR, further suppressed autophagy and decreased COL-I and COL-III expression (Fig. 10).

Collagen fibers exist in the myocardial interstitium, which helps to maintain the structure of the heart. However, excessive collagen production and deposition in the atrial interstitium result in atrial structural remodeling. Atrial structural remodeling not only gives rise to a lasting atrial tissue injury but also affects atrial electrical conduction[41, 42]. Atrial fibroblasts are easily activated by various stimuli and then proliferate and differentiate into myofibroblasts, which secrete amount of collagen that deposits in the atrial interstitium and trigger further atrial remodeling[43]. Numerous studies have documented the link between atrial interstitial fibrosis and AF[3, 4]. Everett *et al.* reported that atrial remodeling occurred in the chronic canine AF model and that electrical and structural dysfunction aggravated the susceptibility to AF[44].

In the cardiovascular system, the alteration of autophagy was detected in various diseases, such as heart failure, cardiac hypertrophy and ischemia-reperfusion injury[45]. Considering the controversial conclusions about autophagy in cardiovascular diseases[46], it is valuable to illustrate the characteristics of autophagy in AF. In the atrium of persistent AF patients, researchers found that autophagic flux and ATG7 protein, an important regulator of autophagy, both increased. A similar phenomenon was observed in a rabbit model with rapid atrial pacing[47]. Another study also reported that autophagy was induced upon endoplasmic reticulum (ER) stress and that suppression of ER stress contributed to the inhibition of autophagy and protection against atrial remodeling in AF models both in vivo and in vitro[14]. As a consequence, they noted that excessive activation of autophagy occurred in advanced AF. Nevertheless, the mechanisms of autophagy in atrial remodeling are still unclear. In the present study, we further confirmed that heavier collagen deposition was accompanied by upregulated autophagy in AF patients' atrium. In the Ang II-perfused mouse model, atrial remodeling was aggravated by heavier collagen deposition in the atrial interstitium. In addition, atrial fibroblast autophagy was increased by colocalization of vimentin and LC3 (Fig. 4). In vivo electrophysiological examination revealed a shortened AERP and increased susceptibility to AF induction in response to Ang II. However, collagen deposition was relieved when autophagy was inhibited by 3-MA. Improved AERP and AF inducibility were also observed when autophagy was inhibited (Fig. 2). The autophagic flux in atrial fibroblasts was also increased in response to Ang II (Fig. 9). In summary, we concluded that suppressing autophagy could ameliorate atrial remodeling induced by Ang II and reduce the susceptibility to AF induction.

Ang II is the principal effector of the RAS, and studies have confirmed that Ang II promotes cardiac interstitial fibrosis by inducing collagen secretion in rat cardiac fibroblasts[48, 49]. Additionally, Ang II can shorten the AERP, which is reversed by candesartan[50]. In the present study, Ang II was used to mimic the

activation effect of the RAS, and it induced COL-I and COL-III expression in atrial fibroblasts by provoking autophagy (Fig. 5). COL-I and COL-III expression was further augmented when provoking atrial fibroblast autophagy with an mTOR inhibitor, rapamycin. In contrast, the opposite phenomenon occurred when blocking autophagy by multiple methods (Fig. 6). In summary, the data suggest that atrial autophagy contributes greatly to Ang II-induced atrial remodeling.

It is well recognized that AT1 is the target through which Ang II exerts its effect. Porrello *et al.* demonstrated that Ang II induced cardiomyocyte autophagy through AT1, and overexpression of AT1 strongly upregulated cardiomyocyte autophagy[24]. That is, AT1 is an upstream regulator of autophagy. What interested us was whether Ang II induced atrial fibroblast autophagy also through AT1. The results showed that autophagy and collagen secretion both decreased when AT1 was blocked (Fig. 8). Meanwhile, candesartan, a specific AT1 inhibitor, restrained atrial fibroblast autophagy induced by Ang II in vivo (Fig. 4). In addition, disturbing AT1 diminished the autophagic flux in atrial fibroblasts (Fig. 9). On the whole, these data showed that AT1 is the key molecular that regulates atrial fibroblast autophagy and collagen secretion induced by Ang II.

It was reported that the ERK signaling pathway was activated in AF patients' atrial tissue and that ACEI inhibited this alteration in ERK[51]. Transgenic mice overexpression the human pro-renin receptor gene exhibited spontaneous AF after 10 months, with serious cardiac fibrosis. Further study found that ERK phosphorylation was specifically increased in cardiac fibroblasts [52]. In brief, these studies suggested that the ERK signaling pathway plays an important role in atrial remodeling and AF. Based on these studies, we found that blocking the ERK signaling pathway not only reduced collagen production, but also restrained autophagy in response to Ang II stimuli (Fig. 7).

Autophagy has a complicated regulatory mechanism involving various signaling molecules. mTOR is a direct negative regulator of autophagy[53]. In vascular smooth muscle cells, autophagy is inhibited by the activated Akt-mTOR signaling pathway[54]. In cardiomyocytes, activated mTOR exerts a protective effect in ischemia/reperfusion injury by restraining autophagy[55]. In summary, mTOR is a pivotal upstream regulator of autophagy in the cardiovascular system. In the current study, Ang II induced fibroblast autophagy by suppressing the phosphorylation of mTOR. In turn, the prevention of AT1 or ERK both rescued the alterations of mTOR (Figs. 7 and 8). In addition, the autophagic flux induced by Ang II in atrial fibroblasts was reduced (Fig. 9). In summary, Ang II induced atrial fibroblast autophagy and further promoted collagen secretion via the AT1-ERK-mTOR signaling pathway in the current study.

From the perspective of translational medicine, the present study identified a potential benefit of pharmacological inhibition of autophagy as a therapeutic strategy in clinical AF. Autophagy is a complicated regulatory system that can be either physiologic or pathologic. The absence of a specific pharmacological inhibitor of autophagy may be an immense deficiency in clinical medicine. The number of enrolled patients was slightly insufficient in this study, but combining previous studies adequately demonstrates that autophagy is upregulated in AF patients' atrial tissues[14, 47]. Although the results show that inhibiting autophagy mitigated collagen deposition and improved atrial remodeling, Ang II

increased atrial fibroblast autophagy in vivo. Little is known about the autophagy changes in atrial cardiomyocytes in vivo. Previous study suggested that autophagy exerted protective effects in cardiomyocytes under stress[56]. Therefore, it is very important to clarify the discrepant roles of autophagy in fibroblasts and cardiomyocytes. Finally, we illustrated the mechanism by which Ang II induced fibroblast autophagy activation in detail. Nevertheless, we did not clarify the downstream mechanism by which enhanced fibroblast autophagy promoted COL-I and COL-III expression in the current study. Our future work will focus on this question. The current study demonstrated the role of autophagy in atrial remodeling and AF from the perspective of atrial fibroblasts. Ang II upregulated fibroblast autophagy and promoted collagen production, further aggravating atrial remodeling.

In conclusion, the current study focused on atrial remodeling after RAS activation. We found that excessive autophagy was concomitant with AF. Ang II aggravated atrial remodeling and susceptibility to AF induction by stimulating atrial fibroblast autophagy and further increasing the expression of COL-I and COL-III. We uncovered the mechanism by which Ang II activated autophagy in atrial fibroblasts (Fig. 10). Prevention of fibroblast autophagy may be an effective way to improve atrial remodeling and AF.

Abbreviations

3-MA: 3-methyladenine; AERP: atrial effective refractory period; AF: atrial fibrillation; AF: atrial fibrillation AF; Ang II: angiotensin II; AT1: angiotensin II receptor type 1; BW: body weight; COL-I: collagen I; COL-III: collagen III; CQ: chloroquine diphosphate salt; CVF: collagen volume fraction; ECG: electrocardiogram; ECM: extracellular matrix; ELISA: Enzyme-linked immunosorbent assay; ER: endoplasmic reticulum; ERK: Extracellular signal-regulated kinase; FBS: Fetal bovine serum; HR: heart rate; HW: heart weight; IVS-d: interventricular septum at end-diastole; IVS-s: interventricular septum at end-systole; LAD: left atrial diameter; LVEF: Left ventricular ejection fraction; LVFS: left ventricular fractional shortening; LVID-d: left ventricular internal dimensions at end-diastole; LVID-s: left ventricular internal dimensions at end-systolic; LVPE-d: left ventricular posterior wall at end-diastole; LVPW-s: left ventricular posterior wall at end-systole; mTOR: a mammalian target of rapamycin; PBS: phosphate buffer saline; Q-PCR: Quantitative real-time polymerase chain reaction; Rapa: Rapamycin; RAS: renin-angiotensin system; siRNA: Small interfering RNAs; SR: sinus rhythm

Declarations

Ethical statement

All animal studies were approved by the Animal Care and Use Committee of Zhejiang University and conformed to the Guide for the Care and Use of Laboratory Animals published by the United States National Institutes of Health (NIH Publication Eighth Edition, 2011).

The informed consent form was obtained from all participants following the guidelines of the Human Research Ethics Committee of Sir Run Run Shaw Hospital of Zhejiang University and conformed to the Declaration of Helsinki.

Availability of data and materials

The datasets are available from the corresponding author on reasonable request.

Conflict of Interests

The authors declare that they have no conflict of interests.

Acknowledgment

We acknowledge Professor Li Lin (Tongji medical college, Huazhong university of science and technology) for technical assistance.

Sources of Funding

This work was supported by the National Natural Science Foundation of China (NO.81900289, awarded to Ruhong Jiang and NO.81570296, awarded to Chenyang Jiang) and the Zhejiang Province Natural Science Foundation of China (LQ17H020003, awarded to Ruhong Jiang).

Authors' contributions

Xudong Xu designed the study, acquired and analyzed the data, and wrote manuscript. Mengmeng Chen designed the study with acquiring and analysis data. Hangyuan Qiu and Kuangshi Zhou assisted in animal experiments. Jun Zhu, Hui Cheng and Yunhe Wang contributed to collect patient's samples and analyze the data, Guosheng Fu assisted in designed the study. Ruhong Jiang and Chenyang Jiang designed the study and edited the manuscript. All authors read and approved the final manuscript.

References

1. Chugh SS, Havmoeller R, Narayanan K, Singh D, Rienstra M, Benjamin EJ, Gillum RF, Kim YH, McAnulty JH, Jr., Zheng ZJ *et al*: **Worldwide epidemiology of atrial fibrillation: a Global Burden of Disease 2010 Study**. *Circulation* 2014, **129**(8):837-847.
2. Burstein B, Nattel S: **Atrial fibrosis: mechanisms and clinical relevance in atrial fibrillation**. *Journal of the American College of Cardiology* 2008, **51**(8):802-809.
3. Boldt A, Wetzel U, Welgl J, Garbade J, Lauschkel J, Hindricks G, Kottkamp H, Gummert JF, Dhein S: **Expression of angiotensin II receptors in human left and right atrial tissue in atrial fibrillation with and without underlying mitral valve disease**. *Journal of the American College of Cardiology* 2003, **42**(10):1785-1792.
4. Frustaci A, Chimenti C, Bellocci F, Morgante E, Russo MA, Maseri A: **Histological substrate of atrial biopsies in patients with lone atrial fibrillation**. *Circulation* 1997, **96**(4):1180-1184.
5. Corradi D: **Atrial fibrillation from the pathologist's perspective**. *Cardiovascular pathology : the official journal of the Society for Cardiovascular Pathology* 2014, **23**(2):71-84.

6. Klionsky DJ: **Autophagy: from phenomenology to molecular understanding in less than a decade**. *Nature reviews Molecular cell biology* 2007, **8**(11):931-937.
7. Levine B, Kroemer G: **Autophagy in the pathogenesis of disease**. *Cell* 2008, **132**(1):27-42.
8. Li J, Zhang D, Wiersma M, Brundel B: **Role of Autophagy in Proteostasis: Friend and Foe in Cardiac Diseases**. *Cells* 2018, **7**(12).
9. De Meyer GR, De Keulenaer GW, Martinet W: **Role of autophagy in heart failure associated with aging**. *Heart failure reviews* 2010, **15**(5):423-430.
10. Kishore R, Krishnamurthy P, Garikipati VN, Benedict C, Nickoloff E, Khan M, Johnson J, Gumpert AM, Koch WJ, Verma SK: **Interleukin-10 inhibits chronic angiotensin II-induced pathological autophagy**. *Journal of molecular and cellular cardiology* 2015, **89**(Pt B):203-213.
11. De Meyer GR, Martinet W: **Autophagy in the cardiovascular system**. *Biochimica et biophysica acta* 2009, **1793**(9):1485-1495.
12. Zhu H, Tannous P, Johnstone JL, Kong Y, Shelton JM, Richardson JA, Le V, Levine B, Rothermel BA, Hill JA: **Cardiac autophagy is a maladaptive response to hemodynamic stress**. *The Journal of clinical investigation* 2007, **117**(7):1782-1793.
13. Hein S, Arnon E, Kostin S, Schonburg M, Elsasser A, Polyakova V, Bauer EP, Klovekorn WP, Schaper J: **Progression from compensated hypertrophy to failure in the pressure-overloaded human heart - Structural deterioration and compensatory mechanisms**. *Circulation* 2003, **107**(7):984-991.
14. Wiersma M, Meijering RAM, Qi XY, Zhang D, Liu T, Hoogstra-Berends F, Sibon OCM, Henning RH, Nattel S, Brundel B: **Endoplasmic Reticulum Stress Is Associated With Autophagy and Cardiomyocyte Remodeling in Experimental and Human Atrial Fibrillation**. *Journal of the American Heart Association* 2017, **6**(10).
15. Schneider MP, Hua TA, Bohm M, Wachtell K, Kjeldsen SE, Schmieder RE: **Prevention of atrial fibrillation by Renin-Angiotensin system inhibition a meta-analysis**. *Journal of the American College of Cardiology* 2010, **55**(21):2299-2307.
16. Unger T, Li J: **The role of the renin-angiotensin-aldosterone system in heart failure**. *Journal of the renin-angiotensin-aldosterone system : JRAAS* 2004, **5 Suppl 1**:S7-10.
17. Campos LA, Bader M, Baltatu OC: **Brain Renin-Angiotensin system in hypertension, cardiac hypertrophy, and heart failure**. *Frontiers in physiology* 2011, **2**:115.
18. Pedersen OD, Bagger H, Kober L, Torp-Pedersen C, Grp TS: **Trandolapril reduces the incidence of atrial fibrillation after acute myocardial infarction in patients with left ventricular dysfunction**. *Circulation* 1999, **100**(4):376-380.
19. Li DS, Shinagawa K, Pang L, Leung TK, Cardin S, Wang ZG, Nattel S: **Effects of angiotensin-converting enzyme inhibition on the development of the atrial fibrillation substrate in dogs with ventricular tachypacing-induced congestive heart failure**. *Circulation* 2001, **104**(21):2608-2614.
20. Renna NF, Lembo C, Diez E, Miatello RM: **Role of Renin-Angiotensin system and oxidative stress on vascular inflammation in insulin resistence model**. *International journal of hypertension* 2013, **2013**:420979.

21. Leung PS: **The peptide hormone angiotensin II: Its new functions in tissues and organs**. *Current protein & peptide science* 2004, **5**(4):267-273.
22. Kumagai K, Nakashima H, Urata H, Gondo N, Arakawa K, Saku K: **Effects of angiotensin II type 1 receptor antagonist on electrical and structural remodeling in atrial fibrillation**. *Journal of the American College of Cardiology* 2003, **41**(12):2197-2204.
23. Cardin S, Li DS, Thorin-Trescases N, Leung TK, Thorin E, Nattel S: **Evolution of the atrial fibrillation substrate in experimental congestive heart failure: angiotensin-dependent and -independent pathways**. *Cardiovascular research* 2003, **60**(2):315-325.
24. Porrello ER, D'Amore A, Curl CL, Allen AM, Harrap SB, Thomas WG, Delbridge LMD: **Angiotensin II Type 2 Receptor Antagonizes Angiotensin II Type 1 Receptor-Mediated Cardiomyocyte Autophagy**. *Hypertension (Dallas, Tex : 1979)* 2009, **53**(6):1032-1040.
25. Jia L, Wang Y, Wang Y, Ma Y, Shen J, Fu Z, Wu Y, Su S, Zhang Y, Cai Z *et al*: **Heme Oxygenase-1 in Macrophages Drives Septic Cardiac Dysfunction via Suppressing Lysosomal Degradation of Inducible Nitric Oxide Synthase**. *Circulation research* 2018, **122**(11):1532-1544.
26. Sun Z, Zhou D, Xie X, Wang S, Wang Z, Zhao W, Xu H, Zheng L: **Cross-talk between macrophages and atrial myocytes in atrial fibrillation**. *Basic research in cardiology* 2016, **111**(6):63.
27. Egom EE, Vella K, Hua R, Jansen HJ, Moghtadaei M, Polina I, Bogachev O, Hurnik R, Mackasey M, Rafferty S *et al*: **Impaired sinoatrial node function and increased susceptibility to atrial fibrillation in mice lacking natriuretic peptide receptor C**. *The Journal of physiology* 2015, **593**(5):1127-1146.
28. Khalil H, Kanisicak O, Prasad V, Correll RN, Fu X, Schips T, Vagnozzi RJ, Liu R, Huynh T, Lee SJ *et al*: **Fibroblast-specific TGF-beta-Smad2/3 signaling underlies cardiac fibrosis**. *The Journal of clinical investigation* 2017, **127**(10):3770-3783.
29. Kanisicak O, Khalil H, Ivey MJ, Karch J, Maliken BD, Correll RN, Brody MJ, SC JL, Aronow BJ, Tallquist MD *et al*: **Genetic lineage tracing defines myofibroblast origin and function in the injured heart**. *Nature communications* 2016, **7**:12260.
30. Xu X, Jiang R, Chen M, Dong M, Liu Q, Cheng H, Zhou K, Chen L, Li M, Jiang C: **Puerarin Decreases Collagen Secretion in AngII-Induced Atrial Fibroblasts Through Inhibiting Autophagy Via the JNK-Akt-mTOR Signaling Pathway**. *Journal of cardiovascular pharmacology* 2019, **73**(6):373-382.
31. Nattel S, Burstein B, Dobrev D: **Atrial remodeling and atrial fibrillation: mechanisms and implications**. *Circulation Arrhythmia and electrophysiology* 2008, **1**(1):62-73.
32. Jalife J, Kaur K: **Atrial remodeling, fibrosis, and atrial fibrillation**. *Trends in cardiovascular medicine* 2015, **25**(6):475-484.
33. Nag AC: **STUDY OF NON-MUSCLE CELLS OF THE ADULT MAMMALIAN HEART - A FINE-STRUCTURAL ANALYSIS AND DISTRIBUTION**. *Cytobios* 1980, **28**(109):41-61.
34. Zeisberg EM, Tarnavski O, Zeisberg M, Dorfman AL, McMullen JR, Gustafsson E, Chandraker A, Yuan X, Pu WT, Roberts AB *et al*: **Endothelial-to-mesenchymal transition contributes to cardiac fibrosis**. *Nature medicine* 2007, **13**(8):952-961.

35. Moore-Morris T, Guimaraes-Camboa N, Banerjee I, Zambon AC, Kisseleva T, Velayoudon A, Stallcup WB, Gu YS, Dalton ND, Cedenilla M *et al*: **Resident fibroblast lineages mediate pressure overload-induced cardiac fibrosis**. *J Clin Invest* 2014, **124**(7):2921-2934.
36. Grobe JL, Mecca AP, Mao H, Katovich MJ: **Chronic angiotensin-(1-7) prevents cardiac fibrosis in DOCA-salt model of hypertension**. *American journal of physiology Heart and circulatory physiology* 2006, **290**(6):H2417-2423.
37. Weber KT, Sun Y, Bhattacharya SK, Ahokas RA, Gerling IC: **Myofibroblast-mediated mechanisms of pathological remodelling of the heart**. *Nature reviews Cardiology* 2013, **10**(1):15-26.
38. Kao C, Chao A, Tsai CL, Chuang WC, Huang WP, Chen GC, Lin CY, Wang TH, Wang HS, Lai CH: **Bortezomib enhances cancer cell death by blocking the autophagic flux through stimulating ERK phosphorylation**. *Cell death & disease* 2014, **5**:e1510.
39. Kinsey CG, Camolotto SA, Boespflug AM, Guillen KP, Foth M, Truong A, Schuman SS, Shea JE, Seipp MT, Yap JT *et al*: **Protective autophagy elicited by RAF–>MEK–>ERK inhibition suggests a treatment strategy for RAS-driven cancers**. *Nature medicine* 2019, **25**(4):620-627.
40. Kim YC, Guan KL: **mTOR: a pharmacologic target for autophagy regulation**. *The Journal of clinical investigation* 2015, **125**(1):25-32.
41. Ausma J, van der Velden HM, Lenders MH, van Ankeren EP, Jongsma HJ, Ramaekers FC, Borgers M, Allessie MA: **Reverse structural and gap-junctional remodeling after prolonged atrial fibrillation in the goat**. *Circulation* 2003, **107**(15):2051-2058.
42. Assayag P, Carre F, Chevalier B, Delcayre C, Mansier P, Swynghedauw B: **Compensated cardiac hypertrophy: Arrhythmogenicity and the new myocardial phenotype .1. Fibrosis**. *Cardiovascular research* 1997, **34**(3):439-444.
43. Nattel S: **Molecular and Cellular Mechanisms of Atrial Fibrosis in Atrial Fibrillation**. *JACC Clinical electrophysiology* 2017, **3**(5):425-435.
44. Everett TH, Li H, Mangrum JM, McRury ID, Mitchell MA, Redick JA, Haines DE: **Electrical, morphological, and ultrastructural remodeling and reverse remodeling in a canine model of chronic atrial fibrillation**. *Circulation* 2000, **102**(12):1454-1460.
45. Kirshenbaum LA: **Regulation of autophagy in the heart in health and disease**. *Journal of cardiovascular pharmacology* 2012, **60**(2):109.
46. Martinet W, Knaapen MW, Kockx MM, De Meyer GR: **Autophagy in cardiovascular disease**. *Trends in molecular medicine* 2007, **13**(11):482-491.
47. Yuan Y, Zhao J, Gong Y, Wang D, Wang X, Yun F, Liu Z, Zhang S, Li W, Zhao X *et al*: **Autophagy exacerbates electrical remodeling in atrial fibrillation by ubiquitin-dependent degradation of L-type calcium channel**. *Cell death & disease* 2018, **9**(9):873.
48. Sadoshima J, Izumo S: **MOLECULAR CHARACTERIZATION OF ANGIOTENSIN-II-INDUCED HYPERTROPHY OF CARDIAC MYOCYTES AND HYPERPLASIA OF CARDIAC FIBROBLASTS - CRITICAL ROLE OF THE AT(1) RECEPTOR SUBTYPE**. *Circulation research* 1993, **73**(3):413-423.

49. Brilla CG, Zhou GP, Matsubara L, Weber KT: **COLLAGEN-METABOLISM IN CULTURED ADULT-RAT CARDIAC FIBROBLASTS - RESPONSE TO ANGIOTENSIN-II AND ALDOSTERONE**. *Journal of molecular and cellular cardiology* 1994, **26**(7):809-820.
50. Nakashima H, Kumagai K, Urata H, Gondo N, Ideishi M, Arakawa K: **Angiotensin II antagonist prevents electrical remodeling in atrial fibrillation**. *Circulation* 2000, **101**(22):2612-2617.
51. Goette A, Staack T, Rocken C, Arndt M, Geller JC, Huth C, Ansorge S, Klein HU, Lendeckel U: **Increased expression of extracellular signal-regulated kinase and angiotensin-converting enzyme in human atria during atrial fibrillation**. *Journal of the American College of Cardiology* 2000, **35**(6):1669-1677.
52. Lian H, Wang X, Wang J, Liu N, Zhang L, Lu Y, Yang Y, Zhang L: **Heart-specific overexpression of (pro)renin receptor induces atrial fibrillation in mice**. *International journal of cardiology* 2015, **184**:28-35.
53. Hosokawa N, Sasaki T, Iemura S, Natsume T, Hara T, Mizushima N: **Atg101, a novel mammalian autophagy protein interacting with Atg13**. *Autophagy* 2009, **5**(7):973-979.
54. Samidurai A, Kukreja RC, Das A: **Emerging Role of mTOR Signaling-Related miRNAs in Cardiovascular Diseases**. *Oxidative medicine and cellular longevity* 2018, **2018**:6141902.
55. Sciarretta S, Volpe M, Sadoshima J: **Mammalian target of rapamycin signaling in cardiac physiology and disease**. *Circulation research* 2014, **114**(3):549-564.
56. Wu X, Qin Y, Zhu X, Liu D, Chen F, Xu S, Zheng D, Zhou Y, Luo J: **Increased expression of DRAM1 confers myocardial protection against ischemia via restoring autophagy flux**. *Journal of molecular and cellular cardiology* 2018, **124**:70-82.

Figures

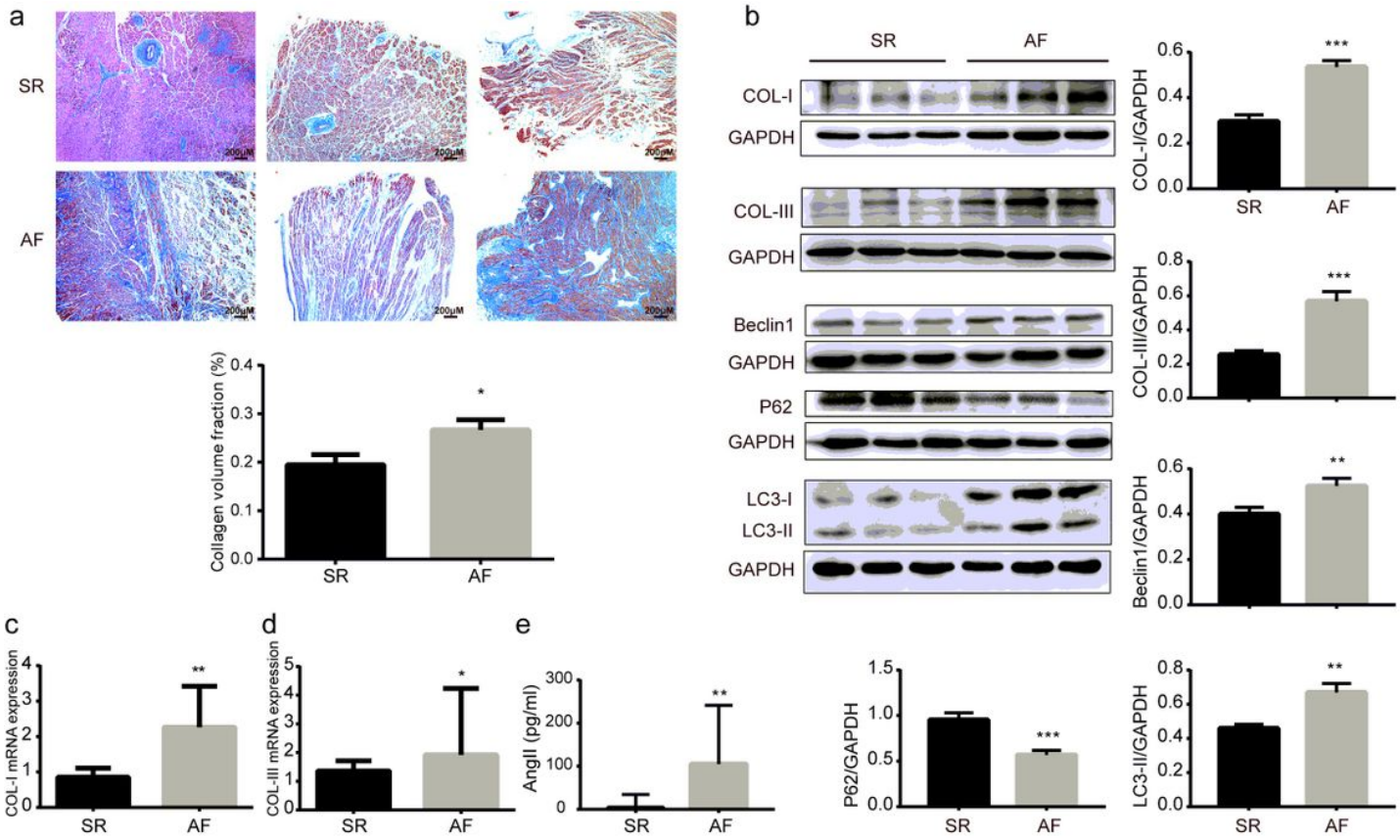

Figure 1

Increased expression of COL-I and COL-III and autophagy in atrial tissues of AF patients. a Representative pictures of Masson's trichrome staining and the collagen volume fraction (Data are expressed as the mean ± SEM, n=16 each group, Scale bar: 200 μm and the original magnification was 40×). b The expression of COL-I, COL-III, Beclin 1, p62 and LC3-II were detected by western blot (Data are expressed as the mean ± SEM, and the most representative pictures and bands are shown; n=16 each group). c The mRNA expression of COL-I in atrial tissues (Data are expressed as the median and interquartile range, n=16 each group). d The mRNA expression of COL-III in atrial tissues (Data are expressed as the median and interquartile range, n=16 each group). e The concentration of Ang II in patients' serum (Data are expressed as the median and interquartile range, n=16 each group). SR: sinus rhythm; AF: atrial fibrillation. *P<0.05 vs SR; **P<0.01 vs SR; ***P<0.001 vs SR.

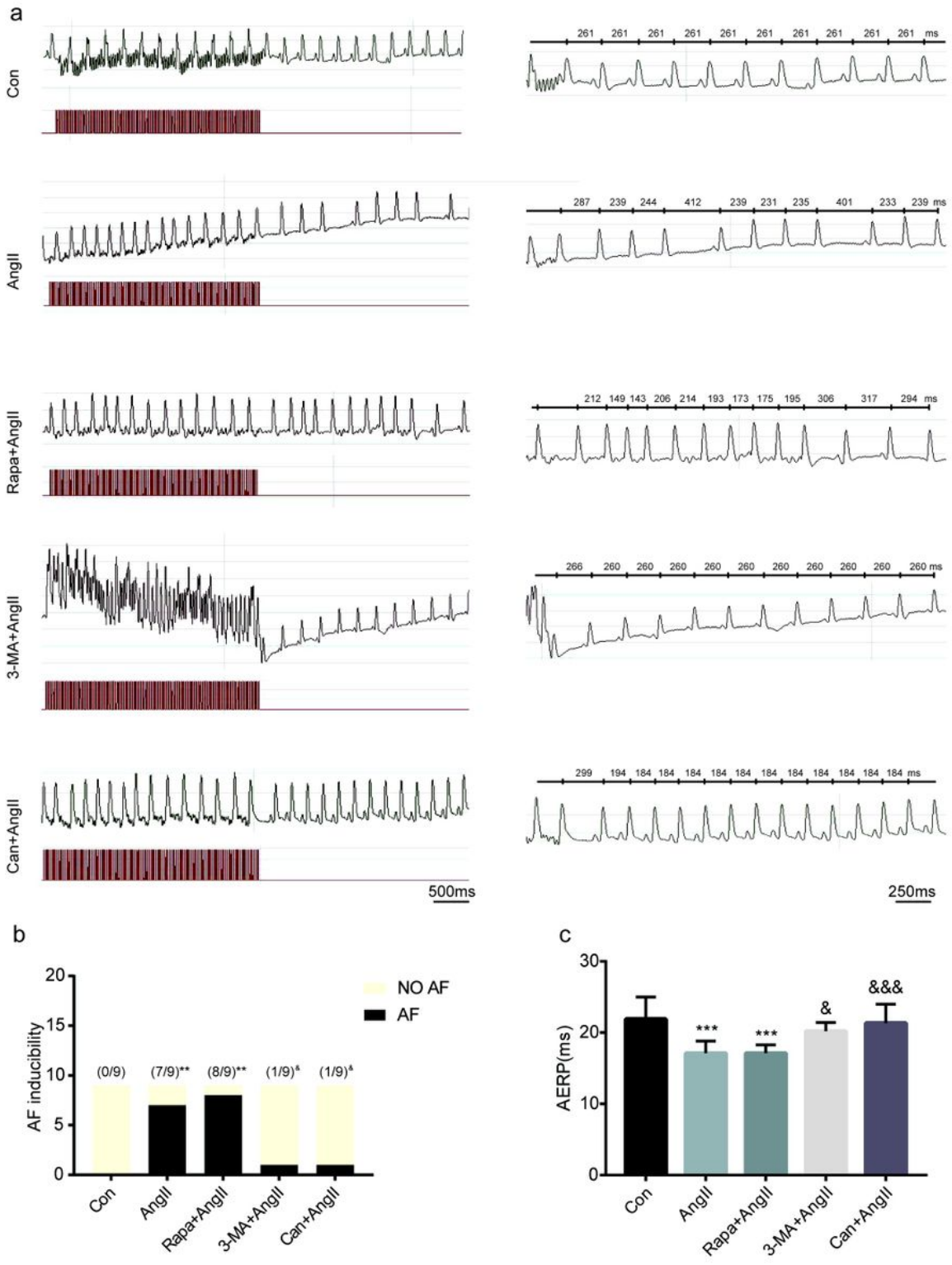

Figure 2

Assessment of AERP and susceptibility to AF in mice. a Representative ECG recordings during intracardiac programmed stimulation in mouse right atrium. b Summary of susceptibility to induced AF in mice. Numbers in parentheses indicate the number of animals that entered AF following burst pacing. c Analysis of AERP in mice. Data are expressed as the mean ± SEM, and the most representative pictures

are shown; n=9 each group. **P<0.01 vs control group (Con); ***P<0.001 vs control group. &P<0.05 vs Ang II group (Ang II); &&&P<0.001 vs Ang II group.

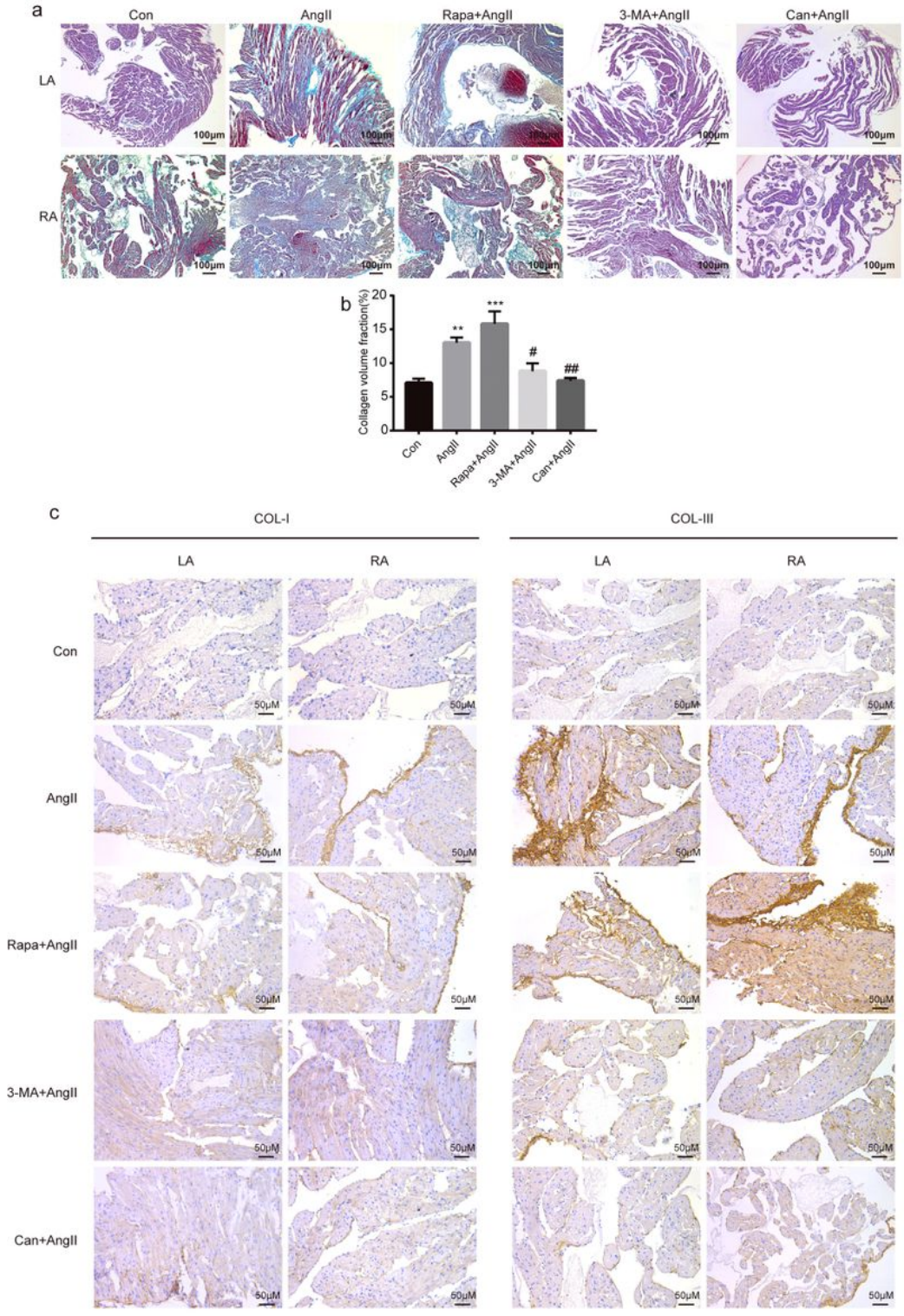

Figure 3

Expression of COL-I and COL-III in mouse atrial tissues. Mouse atrial tissues were obtained from five groups: the control group with vehicle (0.9% saline) infused, the Ang II group with Ang II infused (1.6 mg/kg/day), the rapamycin (Rapa) treatment group with intraperitoneal injection of Rapa (1.5

mg/kg/day) and Ang II infused (1.6 mg/kg/day), the 3-MA treatment group with intraperitoneal injection of 3-MA (35 mg/kg/day) and Ang II infused (1.6 mg/kg/day), and the candesartan (Can) treatment group with oral administration of Can (5 mg/kg/day) and Ang II infused (1.6 mg/kg/day). LA: left atrial; RF: right atrial. a Examples of Masson's trichrome staining of mouse atrial tissues. Collagen was stained with blue. b The statistical results of collagen volume infraction. Scale bar: 100 μm and the original magnification was 100×. c Immunohistochemistry images of COL-I (brown) and COL-III (brown) in mouse atrial tissue. Scale bar: 50 μm and the original magnification was 200×. Data are expressed as the mean ± SEM, n=9 each group. **P<0.01 vs control group (Con); ***P<0.001 vs control group. &P<0.05 vs Ang II group (Ang II); &&P<0.01 vs Ang II group.

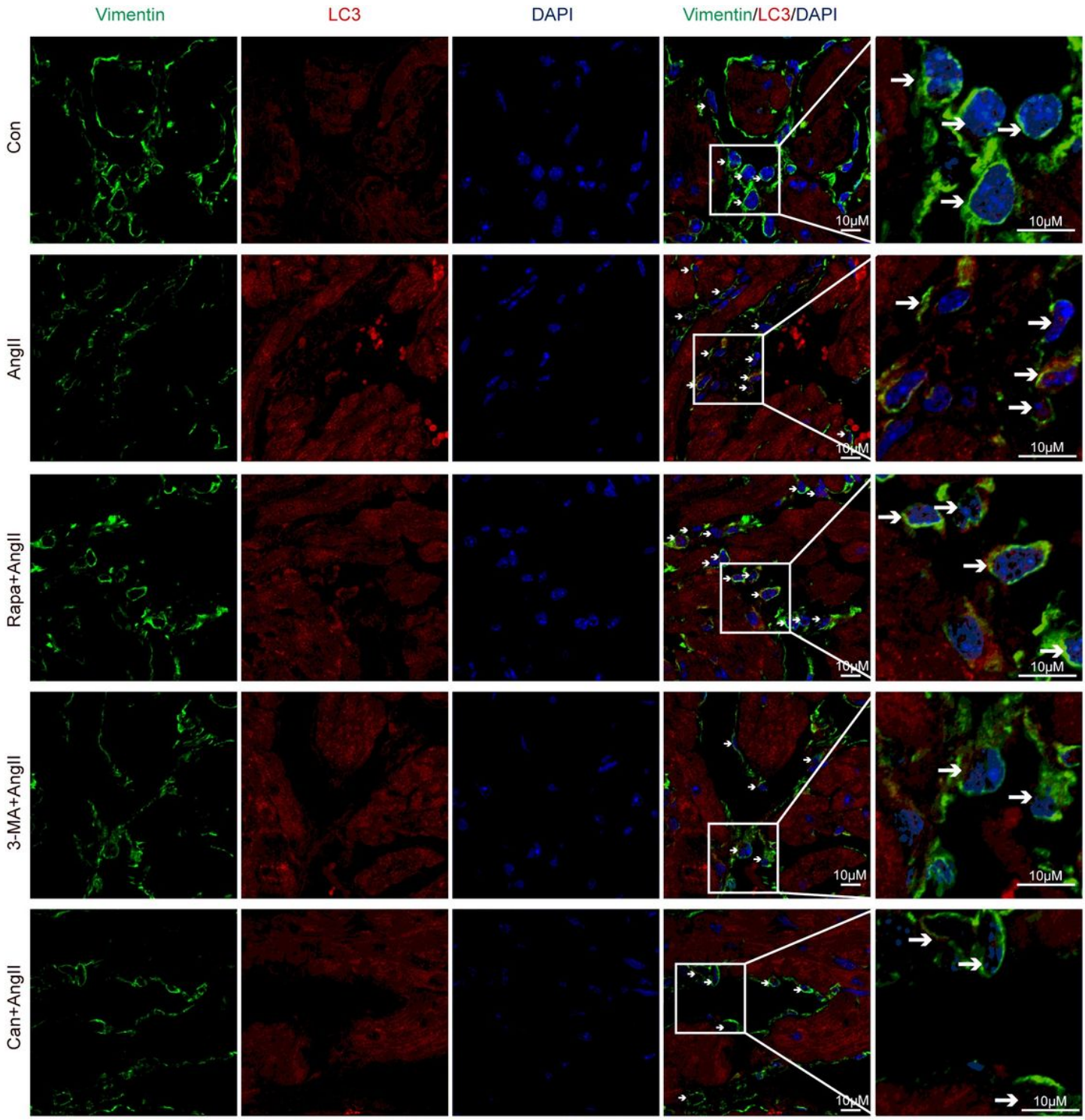

Figure 4

Autophagy in mouse atrial fibroblasts. Mouse atrial tissues were obtained from five groups: the control group with vehicle (0.9% saline) infused, the Ang II group with Ang II infused (1.6 mg/kg/day), the rapamycin (Rapa) treatment group with intraperitoneal injection of Rapa (1.5 mg/kg/day) and Ang II infused (1.6 mg/kg/day), the 3-MA treatment group with intraperitoneal injection of 3-MA (35 mg/kg/day) and Ang II infused (1.6 mg/kg/day), and the candesartan (Can) treatment group with oral administration

of Can (5 mg/kg/day) and Ang II infused (1.6 mg/kg/day). LA: left atrial; RF: right atrial. Vimentin (green), LC3 (red) and nucleus (blue) were stained. Immunofluorescence images show that colocalization of vimentin and LC3 increased in the Ang II and Ang II+Rapa groups and decreased in the 3-MA+Ang II and Can+Ang II groups. n=9 each group. Scale bar: 10 μm and the original magnification was 600× with an oil emulsion.

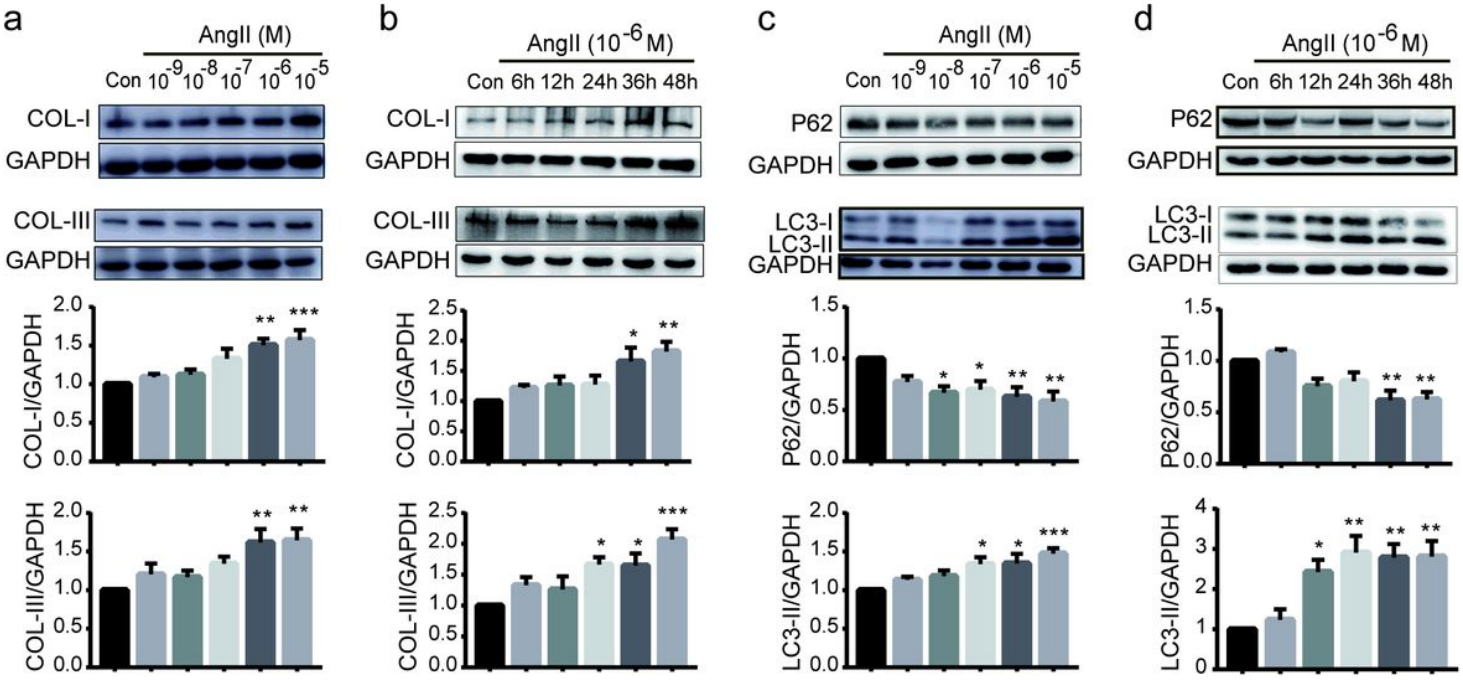

Figure 5

Expression of COL-I, COL-III, p62 and LC3-II in Ang II-induced atrial fibroblasts. Cells were treated with Ang II at different concentrations (10-9 M, 10-8 M, 10-7 M, 10-6 M and 10-5 M) for different times (6, 12, 24, 36 and 48 hours). a Expression of COL-I and COL-III in response to different concentrations of Ang II stimulation for 48 hours. b Expression of COL-I and COL-III at different times of Ang II stimulation at 10-6 M. c Expression of p62 and LC3-II in response to different concentrations of Ang II stimulation for 48 hours. d Expression of p62 and LC3-II at different times of Ang II stimulation at 10-6 M. Data are expressed as the mean ± SEM, and the most representative bands are shown; n=5. *P<0.05 vs control group (Con); **P<0.01 vs control group; ***P<0.001 vs control group.

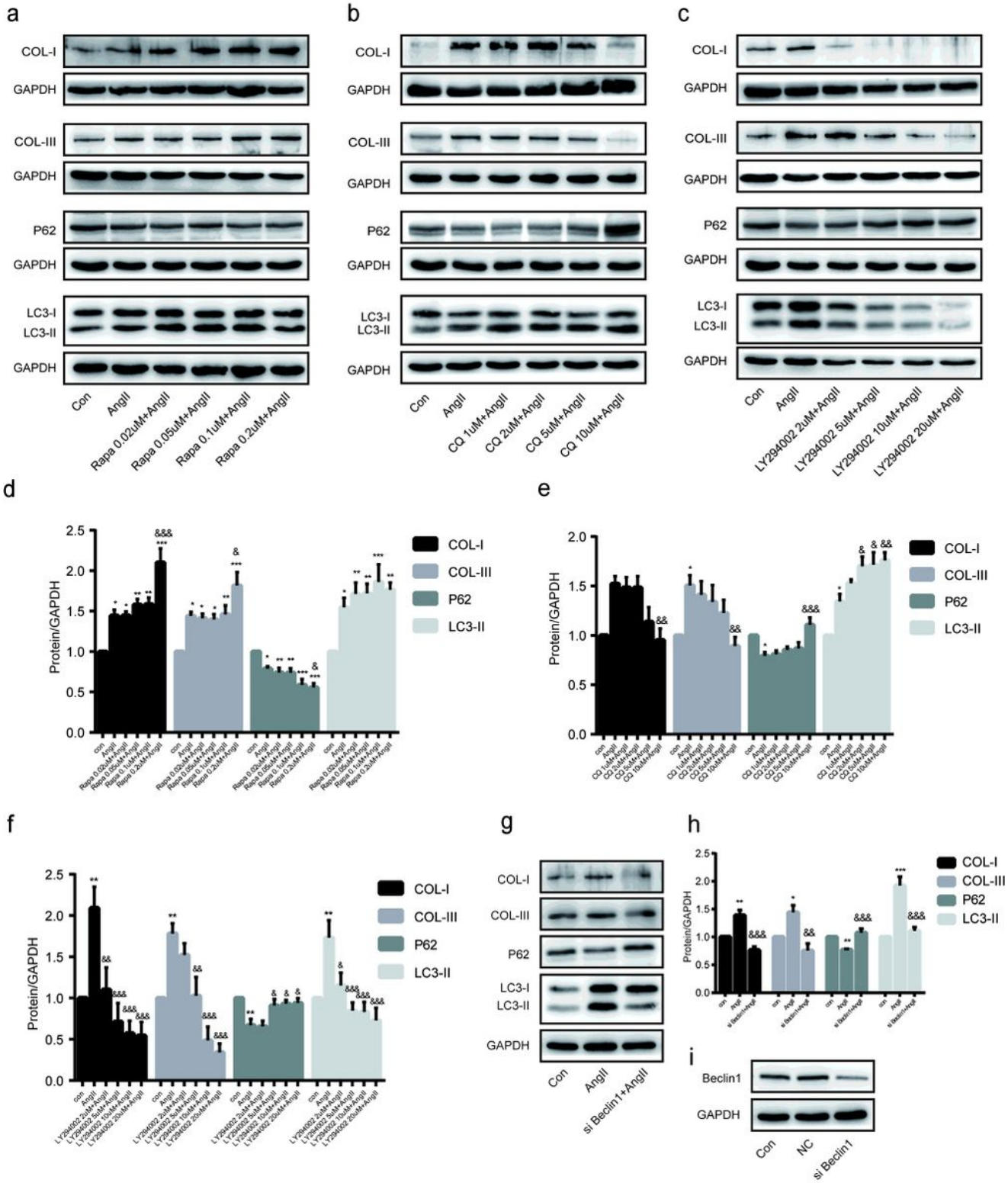

Figure 6

Effects of Rapa, CQ, LY294002 and si-Beclin 1 on the expression of COL-1 and COL-III in Ang II-induced atrial fibroblasts. Cells were pretreated with different concentrations of Rapa, CQ or LY294002 for 1 hour before stimulation with Ang II (10-6 M) for 48 hours or cells pretreated with si-Beclin 1(100 nM) or negative control (NC, 100 nM) for 48 hours before stimulation with Ang II (10-6 M) for another 48 hours. The expression of COL-I, COL-III, p62 and LC3-II was detected by western blot. a, d Atrial fibroblast

autophagy was induced by different concentrations of Rapa. b, e Atrial fibroblast autophagy was suppressed by different concentrations of CQ. c, f Atrial fibroblast autophagy was suppressed by different concentrations of LY294002. i, g, h Beclin 1 was silenced by siRNA. Data are expressed as the mean ± SEM, and the most representative bands are shown; n=5. *P<0.05 vs control group (Con); **P<0.01 vs control group; ***P<0.001 vs control group. &P<0.05 vs Ang II group (Ang II); &&P<0.01 vs Ang II group; &&&P<0.001 vs Ang II group.

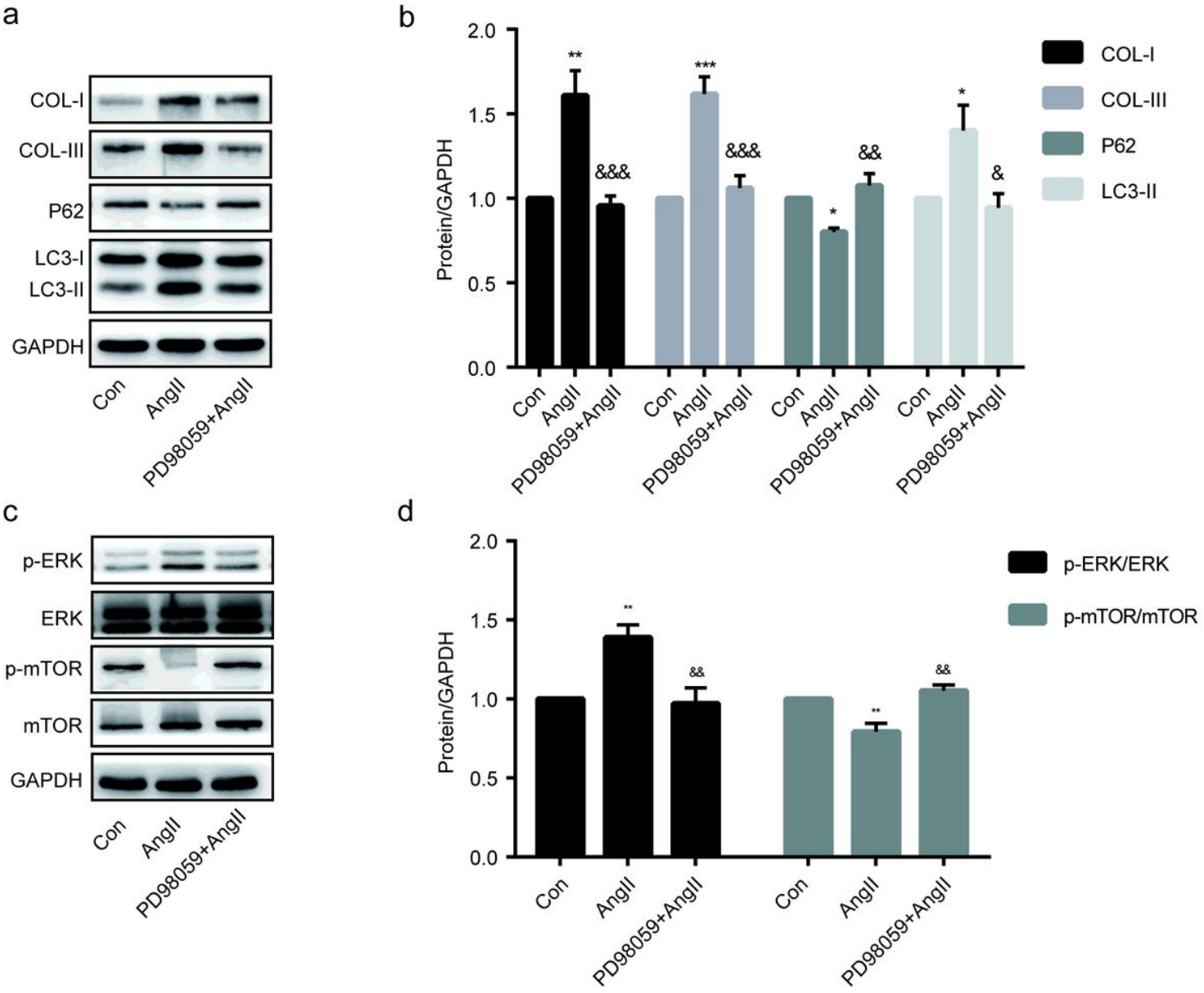

Figure 7

Effects of PD98059 on collagen secretion and autophagy in Ang II-induced atrial fibroblasts. a, b Cells were pretreated with PD98059(10 μM) for 1 hour before stimulation with Ang II (10-6 M) for 48 hours. The expression of COL-I, COL-III, p62 and LC3-II was detected by western blot. c, d Cells were pretreated with PD98059 (10 μM) for 1 hour before stimulation with Ang II (10-6 M) for 20 minutes. The expression of p-ERK/ERK and p-mTOR/mTOR was detected by western blot. Data are expressed as the mean ± SEM, and

the most representative bands are shown; n=5. *P<0.05 vs control group (Con); **P<0.01 vs control group; ***P<0.001 vs control group. &P<0.05 vs Ang II group (Ang II); &&P<0.01 vs Ang II group; &&&P<0.001 vs Ang II group.

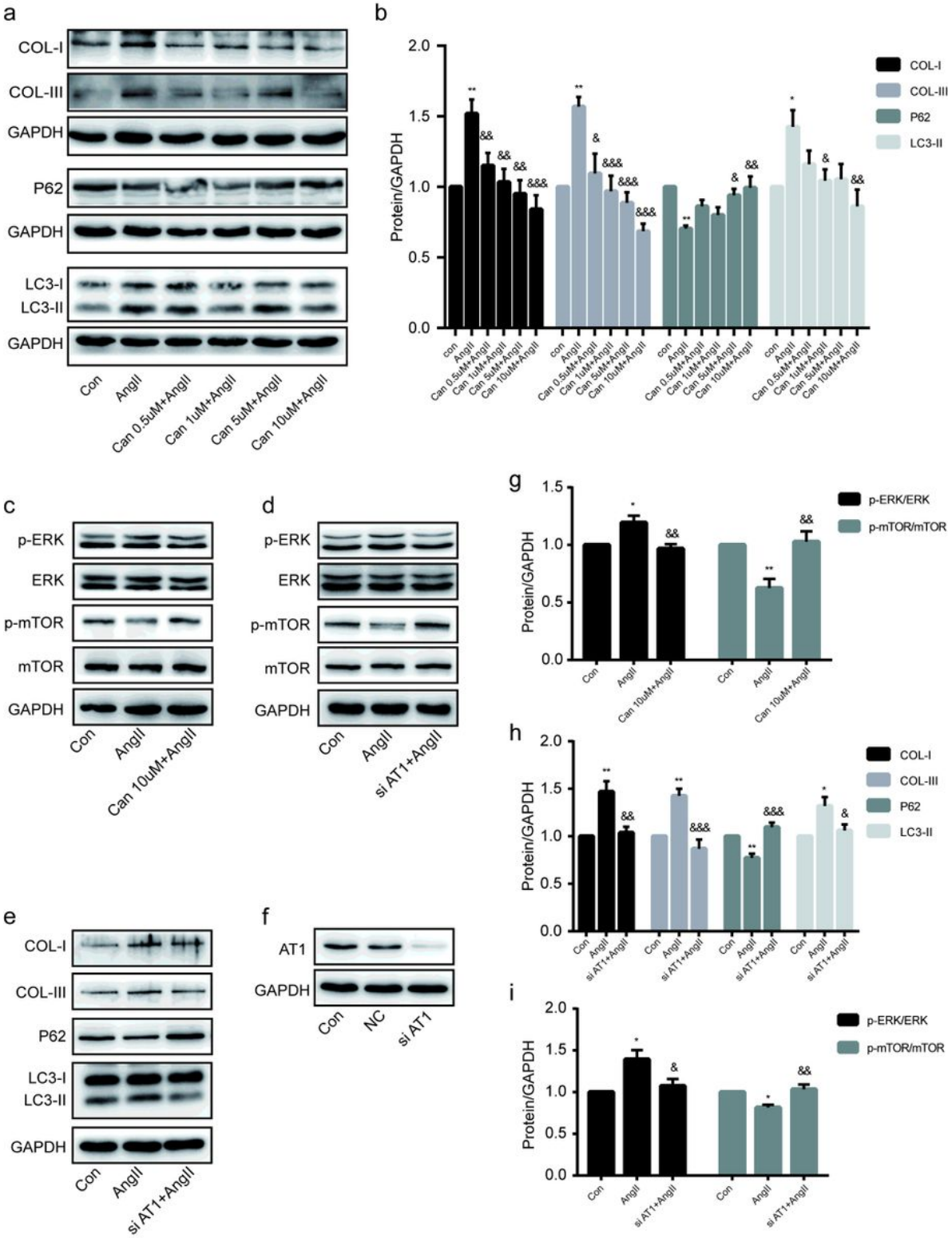

Figure 8

Effects of AT1 on collagen secretion, autophagy and ERK signaling pathway in Ang II-induced atrial fibroblasts. a, b Cells were pretreated with different concentrations of Can (0.5 μM, 1 μM, 5 μM and 10

μM) for 1 hour before stimulation with Ang II (10-6 M) for 48 hours. Protein expression of COL-I, COL-III, p62 and LC3-II was detected by western blot. c, g Cells were pretreated with Can (10 μM) for 1 hour before stimulation with Ang II (10-6 M) for 20 minutes. The expression of p-ERK/ERK and p-mTOR/mTOR was detected by western blot. e, f, h Cells were pretreated with si-AT1(100 nM) or negative control (NC, 100 nM) for 48 hours before stimulation with Ang II (10-6 M) for another 48 hours. The expression of AT1, COL-I, COL-III, P62 and LC3-II was detected by western blot. d, i Cells were pretreated with si-AT1(100 nM) 48 hours before stimulation with Ang II (10-6 M) for 20 minutes. The expression of p-ERK/ERK and p-mTOR/mTOR was detected by western blot. Data are expressed as the mean ± SEM, and the most representative pictures are shown; n=5. *P<0.05 vs control group (con); **P<0.01 vs control group; ***P<0.001 vs control group; &P<0.05 vs Ang II (10-6 M) group; &&P<0.01 vs Ang II (10-6 M) group; &&&P<0.001 vs Ang II (10-6 M) group.

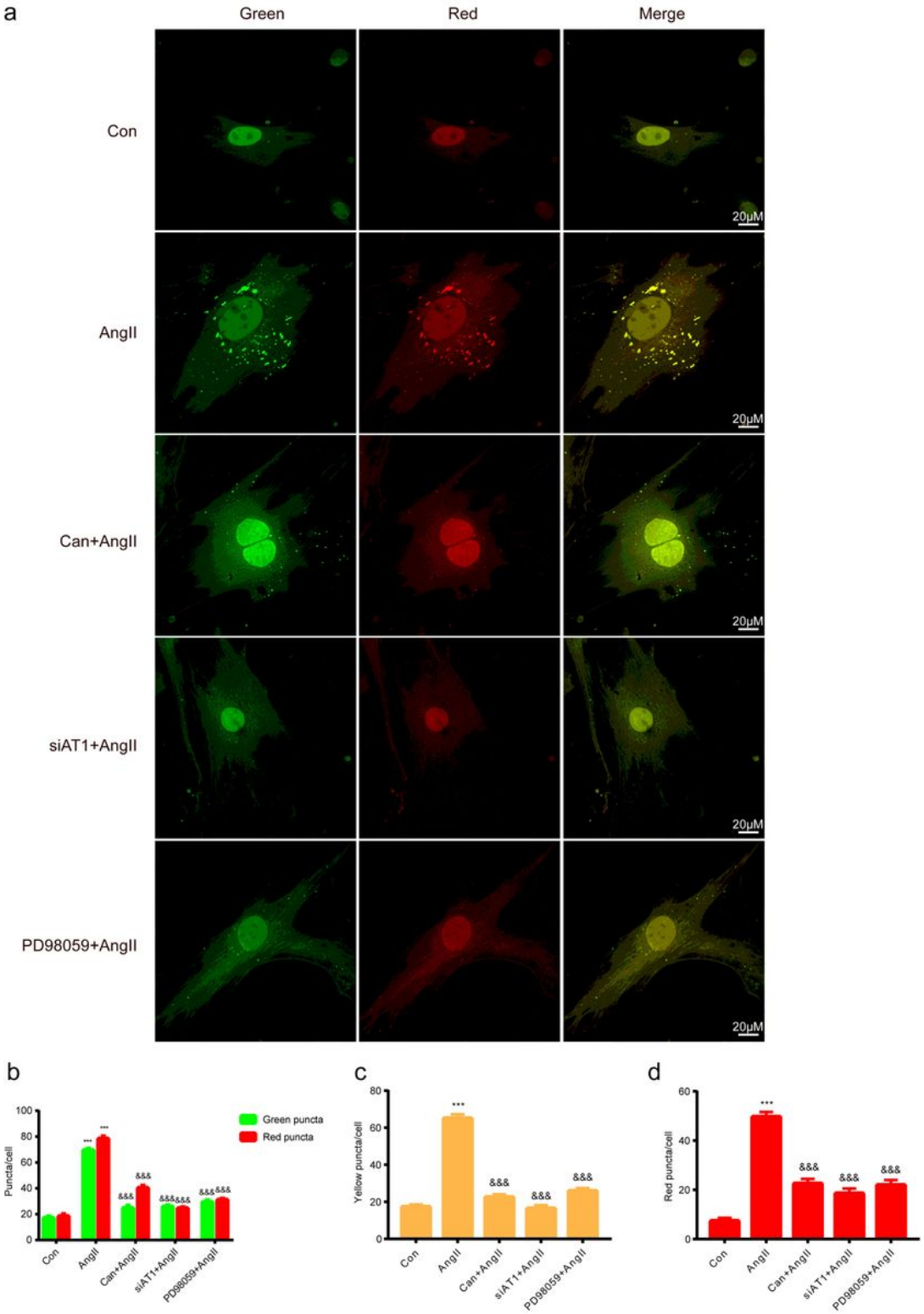

Figure 9

Autophagosomes and autophagic flux in atrial fibroblasts. Cells were transfected with mCherry-GFP-LC3 adenovirus (MOI=100). Then, they were pretreated with Can (10 μM) or PD980559(10 μM) for 1 hour before stimulation with Ang II (10-6 M) for 48 hours. Cells were pretreated with si-AT1(100 nM) for 48 hours before stimulation with Ang II (10-6 M) for another 48 hours. a Representative confocal fluorescence microscopy images (600×) of mCherry-GFP-LC3 localization in atrial fibroblasts. b

Quantitative analysis of green puncta in the green channel and red puncta in the red channel. c, d Quantitative analysis of autophagosomes (yellow puncta in the merged channel) and autolysosomes (red puncta in the merged channel). The average numbers of green, red and yellow puncta were determined by manual counting of fluorescent puncta from at least 30 different fibroblasts in each group. The data are expressed as the mean ± SEM, and the most representative pictures are shown; n=5. Scale bar: 20 μm and the original magnification was 600×. ***P<0.001 vs control group (Con); &&&P<0.001 vs Ang II group (Ang II).

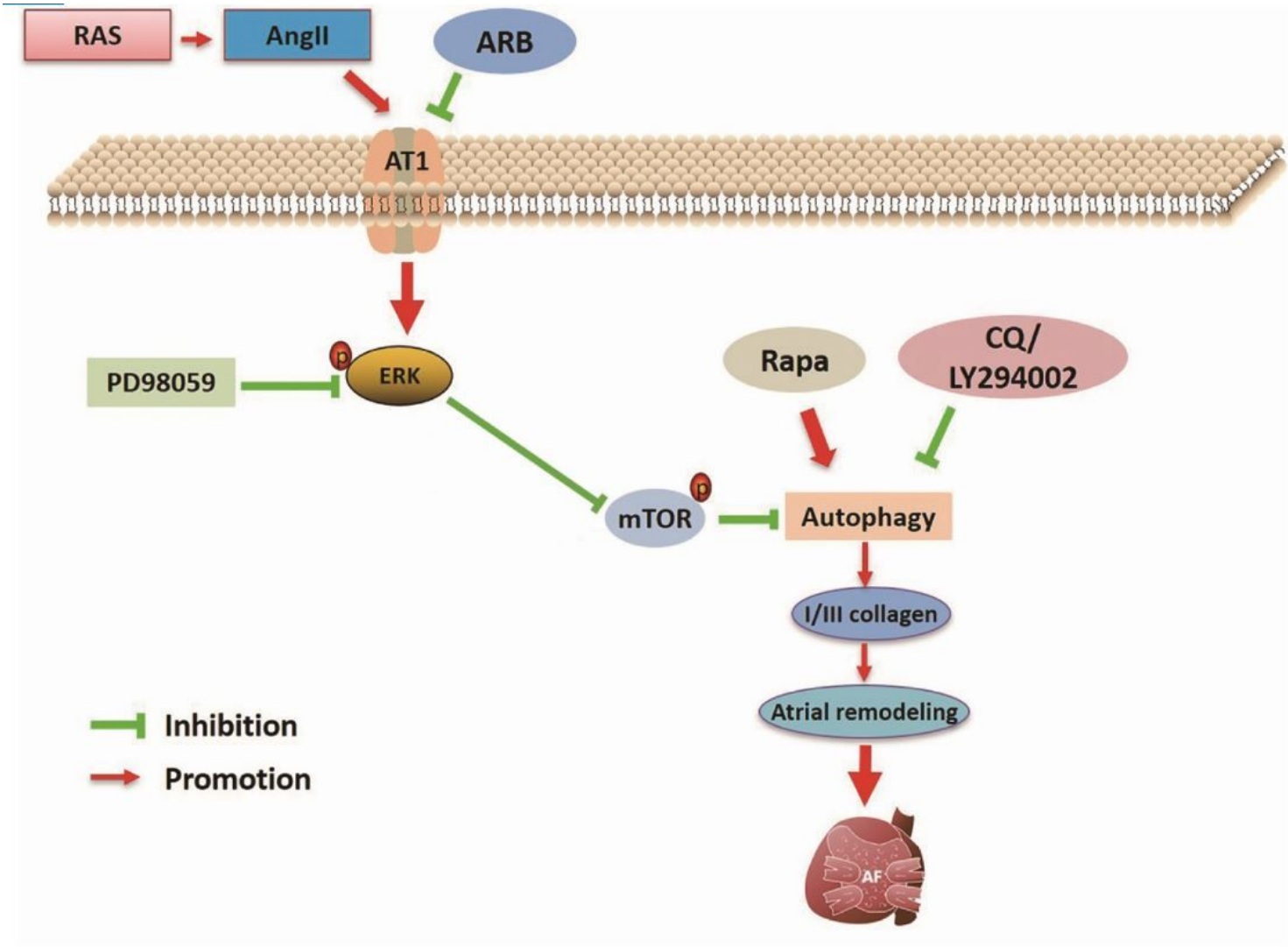

Figure 10

Schematic diagram of Ang II-induced atrial remodeling. Activation of RAS promotes Ang II secretion. Ang II enhances atrial fibroblast autophagy through the AT1-ERK -mTOR signaling pathway. Enhanced atrial fibroblast autophagy aggravates the expression of COL-I and COL-III and further promotes atrial remodeling and susceptibility to AF. RAS: renin-angiotensin system; AT1: angiotensin II receptor type 1; ARB: angiotensin II receptor blocker; Rapa: rapamycin; CQ: chloroquine.